# SYNTHESIS OF GOLD-IRON OXIDE COMPOSITE NANOPARTICLES USING TEA EXTRACT

***Thesis Submitted***

***by***

**Aritri Ghosh**

**(611CH101)**

*Under the guidance of*

**Dr. SANTANU PARIA**

*In partial fulfillment for the award of the Degree of*

**MASTER OF TECHNOLOGY (RESEARCH)**

**IN**

**CHEMICAL ENGINEERING**

**DEPARTMENT OF CHEMICAL ENGINEERING**

**NATIONAL INSTITUTE OF TECHNOLOGY, ROURKELA**

**ROURKELA-769008, ODISHA, INDIA.**

**JANUARY, 2014**

**Department of Chemical Engineering**
**National Institute of Technology**
**Rourkela-769008, Odisha**

---

# CERTIFICATE

This is to certify that the thesis entitled **"SYNTHESIS OF GOLD-IRON OXIDE COMPOSITE NANOPARTICLES USING TEA EXTRACT"** submitted by **Aritri Ghosh** in partial fulfillment for the requirements for the award of the Degree of Master of Technology through Research in Chemical Engineering at National Institute of Technology, Rourkela (Deemed University), is an authentic work carried out by her under my supervision and guidance.

To the best of my knowledge, the matter embodied in the thesis has not been submitted to any other University/Institute for the award of any Degree or Diploma.

**Date:**

**Dr. Santanu Paria**
Department of Chemical Engineering
National Institute of Technology
Rourkela-769008, Odisha

# ACKNOWLEDGEMENT

In pursuit of this academic endeavor, I have received immense support and care from many people, whom I am fortunate to have in my life. I want to thank my family for being patient and always showering me with love and support even in difficult times. I would like to express my sincere gratitude towards my supervisor, Dr. Santanu Paria for his constant motivation and encouragement for pursuing this work. I thank him again for being a support in difficult times and letting me choose this field of topic which helped me increase my knowledge in this field and letting me gain new insight. His association will remain a beacon of light throughout my career.

I gratefully acknowledge the support of my Masters Scrutiny Committee (MSC) members Dr. Sujit Sen, Dr. Sumit Paul for their many useful suggestions and discussions. I would like to express my gratitude to Prof. R. K. Singh, H.O.D Department of Chemical Engineering, for all the facilities provided during the course of my tenure. I would like to thank the entire faculty of Chemical Engineering Department for their constant support throughout my work.

I am also thankful towards Ceramic Engineering Department and Metallurgical & Material Engineering Department, NIT Rourkela for permitting me to use the FESEM and XRD facility during my research work.

I would also like to acknowledge the invaluable support and advice I have received from my current and past lab seniors Dr. Khusi Mukherjee, Dr. Rajib Ghosh Chaudhuri, Dr. Nihar Ranjan Biswal and Mr. K. Jagajjanani Rao. I would like to thank Mr. Naveen Noah Jason, Mr. Krishnendu Chatterjee, Miss Sreerupa Sarkar for their encouragement, help, friendship and especially for making a openhearted atmosphere in the lab. I would also like to thank my fellow lab colleagues Meghna, Siddhartha sir, Rahul, Rohit, Praneeth, Nainsi & Santosh and my friends in the Chemical Engineering Department for their support during my stay at NIT, Rourkela.

**Place: Rourkela**

**Date:** **Aritri Ghosh**

**CONTENTS**

# ABSTRACT

The modernization of current industries and technologies needs day by day smaller nanoparticles in the form of microprocessors, chips, sensors, machines, devices etc. As a result the existing methods of fabrication are slowly becoming obsolete. The fabrication of cytocompatible nanoparticles at small scale requires an inexpensive and promising technique. This work explores the formation of composite nanostructures using gold and iron oxide nanoparticles in a aqueous one-pot synthesis pathway.

Advances in nanoscale level studies have enabled diversification of nanoparticles applications in human healthcare. Several of these biomedical applications comprise use of bioferrofluids i.e. biocompatible colloidal solutions of magnetic nanoparticles, coated with organic or inorganic materials allowing applications specific functionalization. Most of the literature shows usage of complex chemical routes for formation of magnetic nanoparticle, which initiated the pursuit for more environmentally accepted synthesis routes as these produce more biocompatible, stable, and well dispersed nanoparticles in less time than the chemical routes. Among this green route synthesis procedures, usage of plant extract is more suitable as the end product can be easily collected and separated from biomass. The different complexities of magnetic nanoparticles like cytotoxicity, spontaneously oxidizable surface in physiological conditions and less surface functionalization can be modified by addition of gold nanoparticle. In this study we investigate the use of a single plant leaf (Tea) extract as both the reducing agent and a dispersing agent to synthesize iron and gold nanoparticle, and a composite particle of iron-gold nanoparticle, and to characterize the properties of the synthesized nanoparticles.

**Keywords:** Biogenesis of nanoparticles, gold nanoparticles, iron oxide nanoparticles, gold-iron oxide composite nanoparticles, tea extract, one-pot aqueous system.

# List of Figures

# Abbreviation

DLS: Dynamic Light Scattering

DNA: Deoxyribonucleic acid

EDX: Energy-dispersive X-ray spectroscopy

$Fe(NO_3)_3$: Ferric nitrate

$Fe(SO_4)$: Ferrous sulfate

$Fe_2O_3$: Iron oxide

$Fe_3O_4$: Iron oxide

FESEM: Field emission scanning electron microscopy

FT-IR: Fourier Transform infrared

$HAuCl_4$: Chloroauric acid

JCPDS: Joint Committee on Powder Diffraction Standards

MRI: Magnetic resonance imaging

NPs: Nanoparticles

pH: Potential of hydrogen

RNA: Ribonucleic acid

$SiO_2$: Silicone dioxide/silica

TEM: Transmission electron microscope

UV: Ultra-violet

XRD: X-ray diffraction

# Symbols

$\Omega$: Ohm, Electrical resistance

$\pi$: Pi, 22/7

$\lambda$: Lambda $(\pi-2\theta)/(2\pi-2\theta)$

$\theta$: Theta

# Chapter 1

# Introduction

## 1.1 Introduction

In the beginning of the last century scientists were enthralled with the discoveries of sub-atomic particles, and newly discovered elements were included frequently into periodic table, the knowledge of which were applied to either weaponry of mass destruction or towards general well-being of mankind. The knowledge of newer technologies aided researchers in learning the molecular basis of life, to find cure designed for rare diseases, or to invent technologies which paved the ways aimed at studying materials in minuscule level, to be exact in nanoscale level. Nanotechnology is the modern cutting edge inter-disciplinary sciences where chemistry, physics, biology and all other basic sciences are studied in nanoscale level.

The use of nanotechnology without a proper knowledge dates back to a few thousand years. Artisans and potters have long applied gold, silver and other metals in nano form as colorant to produce colored ceramics or tinted glass unaware of the proper scientific reason behind the coloring effect of such metals in nanoscale. Metal nanoparticles exhibit coloring effect owing to a property called surface plasmon resonance due to dimensional change, discovered by Faraday in 1857. The idea of a nanoparticle gathered dust until in 1957, Nobel laureate Prof. Richard P. Feynman introduced the concept to world in his lecture "There's plenty of room at the bottom" (Feynmann, 1957). The idea was a much discussed topic from then on in the medical society for vaccination and drug delivery up to 1960. However technological difficulties limited the idea of nanoparticles from further exploration. The term nanotechnology on the other hand was coined by Japanese scientist Taniguchi in his book published in 1974 (Taniguchi, 1974). The term gained fame and several researchers started looking into the field of sub-micron particles. The science of nanotechnology came into lime light in early 1980s when Eric Dexler started looking in the field of molecular engineering. The research into the field escalated thereafter, with many scientist and research group following in their lead, and looking into the properties and structure of nanoparticles

The term "Nano" stems from Greek semantic meaning 'dwarf'; whereas now it is applied to implicate one billionth unit of a dimension. In conservative vision, nanomaterial has at least one among the three dimension $\leq$ 100 nm, but nanoparticle has the three dimension $\leq$ 100 nm or $100 \text{ X } 10^{-9}$ m. Nanoparticles are intermediary between bulk materials and atomic and molecular structures. When particles are in the nanoscale, they differ from bulk material, which leads to size- dependent enhancement in properties such as reactivity, optical properties in some metal nanoparticles, quantum confinement in semiconductor nanoparticles, super para-magentism in magnetic nanoparticles and thermal stability or mechanical strength in case of some others. The conversion of bulk material to nanoparticles endows the particle with amplified surface area to volume ratio, which in turn increases the availability of surface atoms or a particle.

Arrays of physical, chemical and biological methods have been used to synthesize nanoparticles. Nanoparticles are commonly synthesized using two strategies: “Top-down” and “Bottom-up” (Alivisatos, 1996) approach. In the “Top-down” approach, traditional workshop or microfabrication methods are often applied to cut, mill and shape bulk materials into desired shape and order. Bottom-up approach is generally used for chemical and biological synthesis of nanoparticles as it offers precision, control over the size of the nanoparticle and reduces the cost of the process.

In the beginning, single nanoparticles were studied by scholars, as application of single nanoparticles turned out to be a major concern in miniaturization of electronic or mechanical devices or in bioimaging techniques. Later, further research in the field of nanotechnology around early 1990s publicized that the composite or heterogeneous nanoparticles of two or more materials have considerable superior efficacy than the single nanoparticles. The most notable feature of the magnetic nanoparticles is the super paramagnetic behavior which depends on the dimension of the magnetic nanoparticle. This behavior has been reported by Neel (Neel, 1949) as early as 1949. However further investigation in this field was left unexplored until early 1960s, when the magnetic properties of iron nanoparticles correlating with size and shape of the particle was established by scientists. In the past two decades research on magnetic nanoparticles has experienced a rush in attention due to the new synthesis techniques of magnetic nanoparticle as well as for numerous new applications. In recent times the major usage of magnetic nanoparticles is in bioimaging devices, as a catalyzing agent in fuel industry, in targeted drug delivery, in electrical components as transformers and for sensors and transducer applications. There are several conditions governing the bio-applicability of magnetic nanoparticles like stability of particles in solutions of physical pH, biocompatibility of magnetic nanoparticles which are naturally cytotoxic, degree to which the surfaces of the nanoparticles can be modified to functionalization. Another complexity of applicability magnetic nanoparticles is the materials’ spontaneous oxidizable surfaces. Coating the magnetic particles with a noble metal or a biological molecule can impart the magnetic nanoparticles with the sought after chemical or biomedical properties. Treatment of magnetic nanoparticles with gold nanoparticles provides an intriguing solution to these complexities making the composite an attractive biomedical material as magnetic nanoparticles can be stabilized more proficiently in organic eroding environments and readily functionalized with thiolated organic molecules. There is a growing trend in research activity to fabricate gold-magnetic nanoparticles in different conformations like composite or core/shell to attain hybrid nanostructures with beneficial and serendipitous properties from both the dual gold and magnetic counterparts.

## 1.2 Different Types of Nanoparticles

Nanoparticles can be categorized based on single or multiple materials to simple or composite nanoparticles. Simple nanoparticles are made of single material whereas composite, compositeed or core/shell nanoparticles are of two or more materials. Composite nanoparticles, which are composed of different functional materials, are attracting a lot of interest in recent times due to their combined physicochemical properties and prodigious budding uses in the areas of electronics, photonics, catalysis, biomedical and therapeutics (Caruso, 2001; Roca and Haes, 2008; Yi et. al., 2006; Salgueiriño-Maceira et. al., 2006). The composite nanoparticles exhibit generally a hybrid or compositeed morphology, which can be further manipulated with different charges, reactive groups, or functional surface moieties with heightened stability and compatibility.

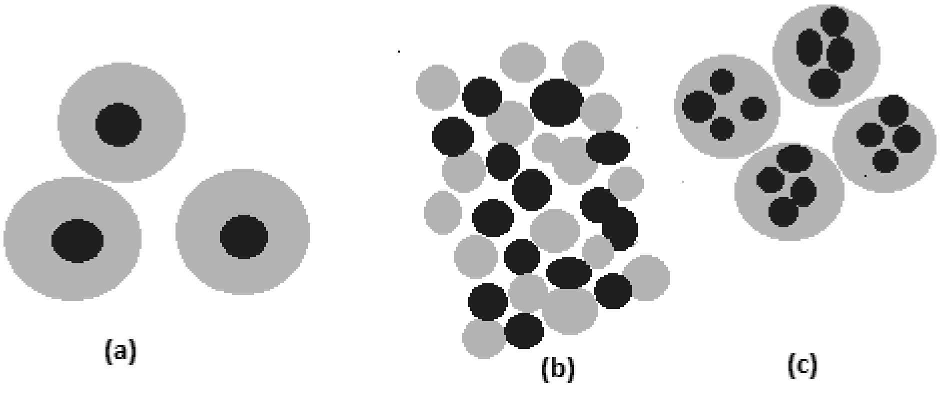

Figure 1.1: Schematic of different types of nanoparticles: (a) Core/Shell nanoparticles, (b) Alloyed nanoparticles, (c) Composite nanoparticles.

The core/shell nanoparticles can be defined as comprising of a core of inner material, and a shell of outer layer material in an enclosing interaction. The core is completely enclosed under the shell material, which diminishes the properties of the core material. The shell material has a lower surface area to volume ratio, and the surface of the shell material can be functionalized with novel ligands to give well–defined applications. Furthermore there can be another shell added to the first shell layer to make a multi-shell nanostructure with single core material. In case of alloyed nanoparticle the precursor materials fuse together forming a complexly structured new material which may possibly show completely different physical and chemical properties from originating materials.

## 1.3 Synthesis Approaches of Nanoparticles

As previously mentioned there are two broad approaches towards synthesis of nanoparticles, "Top-down" and "Bottom-up". These two approaches comprises of different physical, chemical and biological routes of synthesis of nanoparticles. The "Top-down" approach mainly practices different physical methods of nanoparticle synthesis such as: ultraviolet irradiation (Kundu et al., 2007), sonochemistry (Okitsu et al.2007), radiolysis (Meyre et al., 2008), laser ablation (Tsuji et al., 2003) and hydrothermal methods and so on. During physical synthesis procedures atoms are vaporized by condensation on various supports, in which the atoms are rearranged and assembled as small cluster of nanoparticles (Egorova and Revina, 2000). The main advantage of physical approach is that nanoparticles with high purity and desired size and shape can be selectively synthesized (Mafune et al., 2002). Whereas main disadvantages of these methods lies in the usage of complicated instruments, electrical and radiative heating as well as high power consumption, leading to high operating cost.

The trick with "Bottom-up" production of nanoparticles lies in the knowledge of the physical and chemical properties of the materials and swaying them into organize themselves by design into some suitable conformations. "Bottom-up" approach is universally applied in most contemporary chemical and biological ways of nanoparticle synthesis. The most common chemical method of synthesis of nanoparticles is through chemical reduction of material salts in solution phase (Lin et al. 2010). The synthesis routes may follow nucleation or aggregation depending on the condition of the reacting system and reacting components. The commonly used chemicals for these synthesis methods are hydrazine, sodium borohydride, ammonia bromane and hydrogen etc. as reducing agents (Leff et al. 1995; Pileni 1997). For stabilization against oxidation and better dispersity against coalescence of the nanoparticles, several synthetic and natural polymers and copolymers such as rubber, chitosan, cellulose etc. are used. These chemical are sometime hydrophobic, so several chemical or organic solvents like ethylene glycol, dimethyl formamide, ethanol, toluene and chloroform etc. are usually used. These chemicals are hazardous and toxic towards environment and are non-biodegradable. This limits the opportunity to scale up reaction mechanism. Besides the harmful hazardous material present in the nanoparticles make them unsuitable for certain biomedical applications (Shankar et al. 2004a).

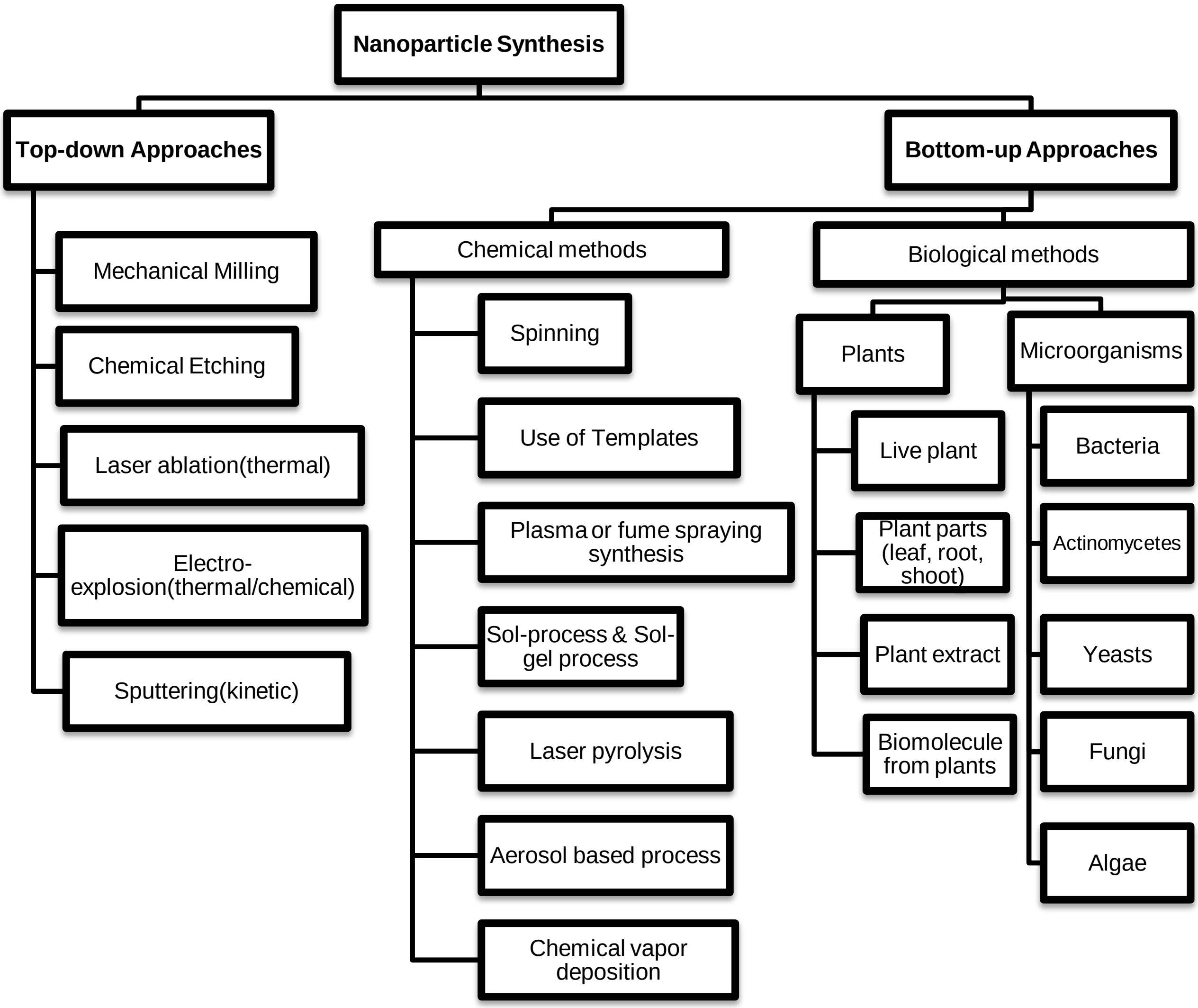

Figure 1.2: Important approaches of nanoparticle synthesis

Biosynthesis of nanoparticles is compatible with green chemistry principles. In biosynthesis, the biomolecules secreted from the biomass or the biomass itself can act as both the reducing agent and the stabilizing agent during the reaction. The biological part may also act as capping agent while forming the nanoparticles. As the reaction can occur in aqueous medium, there is no need to use a different solvent for the reaction process. Biological materials such as plant extract or plant part used in synthesis of nanoparticles normally have a lower electrochemical potential than the chemical reducing agents. Thus biosynthetic process works out well for materials with large positive electrochemical potential favoring the formation of composite nanoparticles.

## 1.4 Motivation of the Work

The main motivation of this study originates from the importance of gold-magnetic composite nanoparticles. Composite nanoparticles are a big favorite material in many industries in current epochs. Gold-magnetic composite nanoparticles are useful for applications in diagnostic, drug delivery, treatment, bio-detection of DNA, RNA, amino acids and proteins, bioseparation, and catalysis activities. For synthesis of gold-magnetic composite or gold, magnetic single nanoparticles, there are various wet chemical methods. But the major disadvantages for those methods are consumption of surfactant or co-surfactant, harmful nature of reducing agent used, purification of the particles and inaptness of nanotheranostic applications. Several of these problems are solved with the practice of biological approaches of nanoparticles synthesis, where it is possible to synthesize nanoparticles in aqueous media without the requirement for surfactant or a dispersing media.

Basic chemical synthesis route for gold nanoparticles includes reduction by using hydrazine, sodium borohydride, ammonia bromane and hydrogen peroxide etc. as reducing agents (Leff et al. 1995; Pileni 1997). Besides the harmful hazardous material present in thus produced gold nanoparticles make them unsuitable for certain biomedical applications (Shankar et al. 2004a). The basic synthesis route of magnetic nanoparticle involves heating iron or other magnetic element's (Ni, Co) precursor solution in slightly alkaline medium in a complex chemical route for formation of magnetic nanoparticles (Gupta et al., 2005). This initiated the search for more environmentally accepted synthesis routes of magnetic nanoparticles in more recent times.

The high electrochemical reduction potential of gold makes it strategic for reduction by several biological materials such as live plant, plant extract and plant polyphenols (Vilela et al., 2012; Sakthivel et al., 2011) led to the synthesis of gold nanoparticles. The synthesis procedures can be further fine-tuned to control the size, shape, structure, stability, bio compatibility and materials attached to the gold nanoparticles. Therefore the main motivation of the work is to develop a biological based technique for one-pot aqueous based synthesis method of both magnetic & gold single nanoparticles, and gold-magnetic composite nanoparticles. Among the magnetic materials iron and iron oxide nanoparticle are most prevalent in multi-disciplinary applications, and gold nanoparticles when coupled with iron or iron oxide nanoparticles; the combination of gold-magnetic composite nanoparticles possesses the advantageous properties from both the materials. Among the different biological systems for synthesis of nanoparticles plant extract is the most commonly used method of choice, as plant extracts are most easy to produce and further purification or identification of functional part of the extract is also possible and they are also beneficial in case of separation of particles and it can work in a multifunctional role of reducing agent, dispersing media or also as capping agent.

### 1.5 Organization of thesis

The thesis has been divided into six chapters. Chapter-1 consists of the basic introductory literature. Here a brief history and introduction to nanotechnology is given followed by general information on nanoparticles, types, synthesis approaches. Chapter-2 is an exhaustive literature review on biogenesis of nanoparticles, different types of gold-magnetic nanocomposite structures along with the applications. Chpater-3 deals with the synthesis of gold nanoparticles by using plant leaf extract in our case tea leaf extract in a one-step process. In chapter-4 the same leaf extract is used to synthesize iron oxide nanoparticles in a one-step process and a possible mechanism is explored. Chapter-5 describes the synthesis of gold-iron oxide composite nanoparticles and possible mechanism of the synthesis process. Chapter-6 concludes the research works described in the previous chapters and also contain few suggestions for future work.

# Chapter 2

# Background Literature

## 2.1 Introductions

Composite nanoparticles are defined as the nanomaterials with composite structure which are constituted by two or more components of nanoscale with special physical and chemical properties. Mutual contact interfaces exist between the respective components. The components with different functionalities have significant and strong mutual coupling effect on a nanometer scale. Thus the composite nanoparticles are not simply integrating these components' effects. The composite nanomaterials not only enhance intrinsic performance significantly, but also show a variety of novel features and break the limitations of single-component's properties. From a scientific point of view the composition and the atomic order of the aggregates, in addition to size, are pivotal factors in determining their properties and functionalities, while the nanoscale regime confers to them structural and electronic degrees of freedom which are inaccessible to bulk materials. The composite nanoparticles have demonstrated excellent prospects in some important areas, such as development of new functional materials, effective utilization of new energy, wastewater treatment and biochemical and biomedical application etc.

Gold-magnetic composite nanoparticles are well known for their unique dual properties and application in many fields such as electronics, biomedical, pharmaceutical, optics and catalysis and many other applications. The synthesis approach for the production of composite nanoparticles has also changed over the years, from complex chemical routes it has now reached an age where green routes of synthesis of nanoparticles are used for producing biocompatible composite nanoparticles for further applications.

This chapter of the thesis mainly focuses on the review of composite nanoparticle especially focusing on gold-iron oxide composite nanoparticles, their structural classification and synthesis approaches and applications. This chapter also sheds light on the synthesis approaches in green route synthesis procedures, describing in a generalized way with classification of approaches and plausible mechanism of formation.

## 2.2 Composite Nanoparticles

Nanoparticles are categorized based on single or multiple materials present into simple and core/shell or composite nanoparticles. Simple nanoparticles are made from a single material, whereas composite materials are as the name indicates are composed of two or more materials in close interacting condition with each other. Composite nanoparticles can be classified based on the materials present or on the structural basis. As we are concentrating on gold-iron oxide composite nanoparticles the classification discussed here is based on the structure of the composite nanoparticles. They can be broadly classified in two main categories monodispersed nanocomposites and aggregates. The monodispersed types of nanocomposites can be further classified into five categories as described below. It is noteworthy that monodispersed nanoparticles have drawn more attention from chemists and material scientists due to their promising reproducibilities and reliable characteristic properties for further modification and applications. Facile synthetic methods have been recently developed for the synthesis of monodispersed Au and $Fe_xO_y$ nanoparticles with tunable sizes as well as post modifications for Au–$Fe_xO_y$ linkages and bioconjugations.

### 2.2.1 Classification & Synthesis Approaches

Composite types of nanoparticles are broadly divided into monodispersed and aggregate nanoparticles in the basis of configuration. The different synthesis approached of along with the different classes of composite nanoparticles is described below.

#### 2.2.1.1 Monodispersed Composite Nanoparticles –

##### 2.2.1.1.1 Core/satellite structures

One of the common structures of Au– $Fe_xO_y$ nanocomposites is the core/satellite structure. This structure possesses a single core with the attachment of numerous smaller nanoparticles, i.e., satellites, linking by covalent bonds or supramolecular interactions. Remarkably, Au@$Fe_xO_y$ or $Fe_xO_y$@Au core/satellite structures sometimes are the key intermediates for conversion to core/shell or multilayer composite structures with distinctive features. The core/satellite nanocomposite consists of a residually uncovered core surface which is eligible for further functionalization or achieving specific properties from the core material. Moreover, this structure, which consists of numerous peripheral satellite nanoparticles, possesses a high surface area of satellite material, benefiting for specific functions, e.g., catalysis, uniform shell formation, etc.

The most commonly reported core/satellite structure in the literatures is the $Fe_3O_4$@Au because of the well-established, facile syntheses of the $Fe_3O_4$ core (Jeong et al., 2007) (~50–300 nm) by solvothermal reactions and Au nanoparticle (~2–20 nm) by Au anion reduction (Tian &

Tatsuma, 2005). Magnetic γ-$Fe_2O_3$ or $Fe_3O_4$ nanoparticles of various sizes could be coated with uniform silica shells (~3–50 nm of thickness) via sol–gel reactions and also functionalized with peripheral amine/ammonium groups. Negatively charged citrate-coated Au nanoparticles could be attached onto the positively charged ammonium-functionalized $Fe_xO_y$@$SiO_2$ nanoparticles via electrostatic interactions, yielding the $Fe_xO_y$@$SiO_2$@Au core/shell/satellite nanocomposite structures. FexOy nanoparticles could be coated with positively charged organic polymers and then subjected to the attachment of negatively charged citrate-coated Au nanoparticles. The resulting $Fe_xO_y$@polymer@Au core/shell/satellite nanocomposite structure (Figure. 2.1) is considered more stable than the $Fe_xO_y$@$SiO_2$@Au structure due to multivalent electrostatic interactions between the flexible polymer and Au nanoparticles. However, it was found that some Au nanoparticles on the flexible polymer support might be agglomerated to form larger aggregates (Amal et al., 2009, Qi et al., 2010)

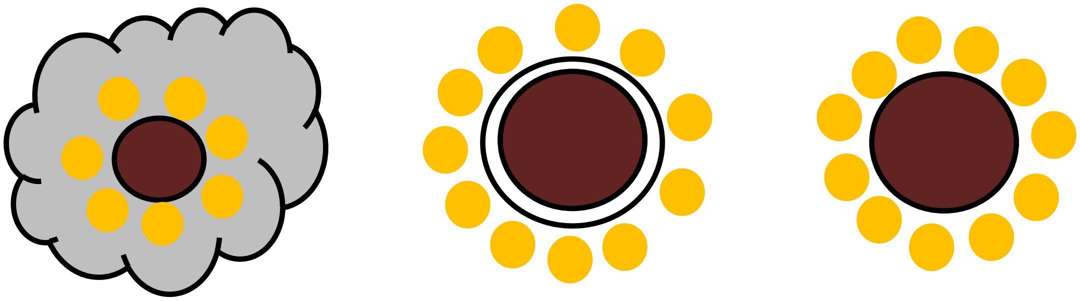

**Figure 2.1:** Schematic representation of $Fe_xO_y$@Au core/satellite structures prepared by using different linkers via electrostatic interactions polymer, amine functionalized organosilica, lysine respectively.

Xuan et al. ( Xuan et al., 2009) and Wang et al. (Wang et al., 2008) reported that an in situ polymerization of monomers (aniline, allylamine, etc.) on $Fe_xO_y$ nanoparticles followed by addition of Au nanoparticles could successfully yield monodispersed $Fe_xO_y$@polymer@Au core/shell/satellite nanocomposite structures. Small molecules such as amino acid lysine, cysteine also serves as a linker between the $Fe_xO_y$ nanoparticle core and Au nanoparticle satellites (Wang et al., 2010). The carboxylic end of lysine and the thiol group of lysine acts as the linker between the iron oxide core and gold nanoparticles. Although this method is restricted by its specific reaction condition, the narrow polydispersity and characteristic structural features render it worth further investigations.

### 2.2.1.1.2 Core/shell structures

Core/shell nanocomposite is defined as a nanoparticle with a single core and fully covered with a shell coating. In contrast to the core/satellite structure, the surface of the core is completely buried under the shell, diminishing the properties of the core material. Moreover, a lowered surface area to volume ratio of the shell material would be obtained, comparing to the core/satellite structure. The surface of the uniform core/shell nanocomposite could be further functionalized with new ligands to give well-defined structures. Uniform Au@ $Fe_xO_y$ core/shell and Au@ $Fe_xO_y$ cluster/shell composite structures were seldom investigated due to the synthetic challenge and the inactivated properties of the Au core inside the $Fe_xO_y$ shell. On the other hand, uniform $Fe_xO_y$ @Au core/shell composite structures have been widely used towards many different applications.

Generally there are two methods to synthesize $Fe_xO_y$ @Au core/shell composite structure either by coating a uniform Au layer based on a $Fe_xO_y$ @Au core/satellite composite or directly coating the $Fe_xO_y$ core (Serpell et al., 2005). The coating of an Au shell to any material requires the reduction of $HAuCl_4$.

When $Fe_xO_y$ @Au core/satellite composites are isolated or prepared in situ, the satellite Au nanoparticles on the $Fe_xO_y$ core will serve as nucleation sites for coating of the Au shell with $Au^{3+}$ and a reducing agent. This strategy is capable with a wide range of sizes of $Fe_xO_y$ core particles from 634 to 100 nm with different special morphologies such as rice (Wang et al., 2006) and cube (Levin et al., 2009) as well. In order to reduce $HAuCl_4$ to metallic Au, various reducing agents such as formaldehyde with potassium carbonate , hydroxylamine ($NH_2OH$) 40 were reported in order to facilitate the process. These reduction procedures require careful control of temperature and sonication otherwise aggregates and rough surfaces may be formed. The concentration of Au precursor and the reducing agent concentration play a crucial role in formation of a uniform Au shell layer.

Besides the use of small Au nanoparticles as a nucleation site for coating Au shell onto the $Fe_xO_y$ core, Au shell could be formed directly on the $Fe_3O_4$core surface (Zeng et al., 2008, Chung et al., 2007) Basically, the $Fe_3O_4$core surface has to be modified with functional groups which could be served as templates for nucleation of Au. For example, small $Fe_3O_4$nanoparticles (5–15 nm) (Zhong et al., 2008) were first synthesized by the reduction of $Fe(acac)_3$ by 1,6-hexadecanediol in the presence of capping agents—oleic acid (OA) and oleylamine (OAm). Then, the $Fe_3O_4$nanoparticle served as seeds for the coating of the Au shell. It should be noted that OAm is a crucial surfactant, providing an amine functional group as a template to attach $Au^{3+}$ ions. Followed by the reduction of $Au(CH_3COO)_3$ by 1,6-hexadecanediol in the presence of capping agents, monodispersed $Fe_xO_y$@Au core/shell composites could be synthesized with a 5–15 nm core and 0.5–2 nm Au shell thickness. Lim et al. also employed a similar approach to construct a $Fe_3O_4$@Au core/shell structure. OAm could also be functioned as a reducing agent to reduce $HAuCl_4$ and stabilize the Au shell formed (Katoaka et al., 2010) Using OAm as the reducing agent would result in non-uniform thickness of coating on the γ-$Fe_2O_3$ nanoparticles.

#### 2.2.1.1.3 Multi-layer Composite Structures

The previous two structural forms of nanocomposites are basically bi-composite materials. But many research groups are interested in investigating the scope of bi-composite materials by introducing more layers of material on them in a view to synthesize "all in one" nanocomposites. Silica layer coating is common after the synthesis of the $Fe_xO_y$ core due to its ability to stabilize the $Fe_xO_y$ core and prevent its aggregation. To coat a silica layer onto $Fe_xO_y$ nanoparticles, tetraethylorthosilicate (TEOS) is typically used for a sol–gel reaction. During the synthesis of Au–$Fe_xO_y$ nanocomposites, the silica layer is introduced in order to increase the size and stability of $Fe_xO_y$. For example, Huang et al. reported that $Fe_xO_y$ nanoparticles are first coated with a silica layer before constructing the core/satellite and core/shell structures (Huang et al., 2009)

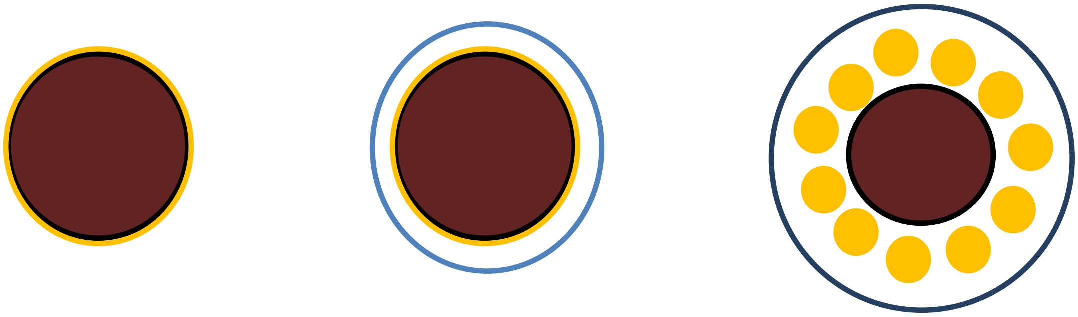

**Figure 2.2:** Schematic representation of core/shell $Fe_xO_y$@Au nanoparticles, core/shell $Fe_xO_y$@Au@$SiO_2$ nanoparticles and $Fe_xO_y$@Au-core-satellite@ $SiO_2$ multi-layer $Fe_xO_y$@Au nanoparticles respectively.

Double-layered Au shell could be constructed by means of coating a silica layer on the inner Au shell, followed by another coating of Au shell on the silica layer (Lee et al., 2008) Core/satellite structure constructed by an amine-functionalized sphere is unstable as discussed before. Bardhan et al. reported the stabilization of satellite Au nanoparticles by coating a silica layer. Not only does the silica layer stabilizes the Au nanoparticles, but also immobilizes fluorophore ICG at the same time. This broadens the scope of using a silica layer in synthesizing multi-layered composite materials. In the coating of a silica layer followed by an itching process, silica layer served as a scaffold in constructing hollow type composite nanoparticles. As reported by Yeo et al., the $Fe_3O_4$@Au core/satellite composite is coated with a silica layer. By selective etching of the $Fe_3O_4$core with $NaBH_4$, hollow silica nanoparticles embedded with Au nanoparticles were synthesized (Lee et al., 2010). Figure 2.2 illustrate the schematic of multi-layer $Fe_xO_y$@Au composites.

#### 2.2.1.1.4 Nano-dumbbell Structures

Au–$Fe_xO_y$ dumbbell nanocomposites are distinct monodispersed nanoparticles that are composed of one Au nanoparticle and one $Fe_xO_y$ nanoparticle, bonded interfacially. There are generally two strategies to synthesize Au–$Fe_xO_y$ dumbbell nanocomposites. The first synthetic strategy involves the synthesis of Au nanoparticles, followed by the deposition of one $Fe_xO_y$ nanoparticle onto each Au nanoparticle. The second synthetic strategy involves a simultaneous decomposition of Au and Fe complexes to form Au–$Fe_xO_y$ dumbbell nanocomposites.

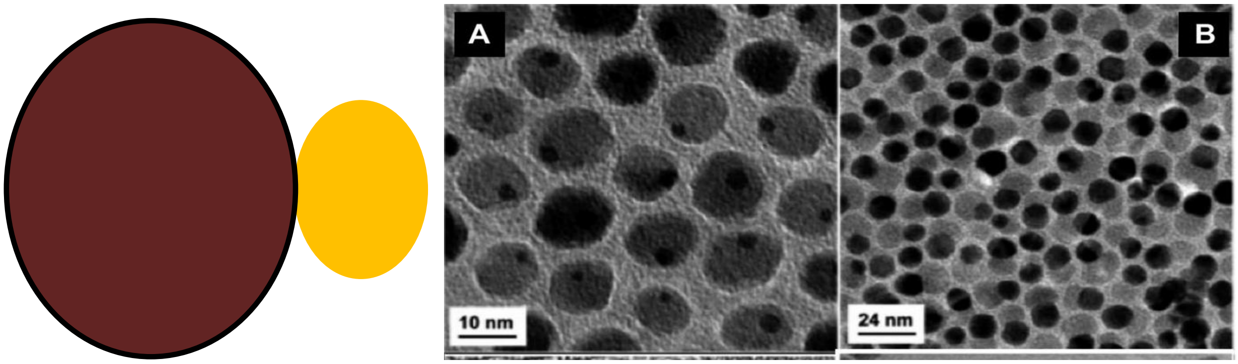

**Figure 2.3:** Schematic and TEM images of Au-$Fe_xO_y$ dumbbell nanocomposites (Yu et al., 2005).

In the Figure 2.3 a schematic of the dumbbell nanoparticles with some examples are shown. For the first synthetic strategy, OAm-coated Au nanoparticles are first synthesized separately. These Au nanoparticles are then reacted with Fe complexes, whereas the newly formed $Fe_xO_y$ nanoparticle is deposited onto the Au surface. There are generally two Fe complexes employed, i.e., iron pentacarbonyl ($Fe(CO)_5$) and iron-oleate complex ($Fe(OL)_3$). $Fe(CO)_5$ would be decomposed upon refluxing with Au nanoparticles, 1-octadecene, OA and OAm at 300˚C, yielding metallic Fe. In order to obtain $Fe_xO_y$, the product has to be exposed and oxidized in atmospheric air, yielding the product Au–$Fe_xO_y$ dumbbell nanocomposites. It was reported that the size of the particles could be tuned from 2 to 8 nm for Au and 4 to 20 nm for $Fe_3O_4$.(Yu et al., 2010) In the study performed by Manna et al., it was discovered that by varying the reaction temperature from 190 to 320˚C and the reaction time from 30 min to 4 h, the nanoparticles will evolve from core/shell nanoparticles into various metal–metal oxide core/shell morphologies and then to heterodimers (Manna et al., 2011) On the other hand, when the $Fe(OL)_3$ complex is employed as the precursor, Au–$Fe_xO_y$ dumbbell nanocomposites could be obtained by simply refluxing a mixture which contains $Fe(OL)_3$, Au colloid dispersion (synthesized by reducing $HAuCl_4$ with tertbutylamine borane complex), OA, OAm, and 1-octadecene. The size of the synthesized nano-dumbbells ranges from 12 to 16 nm. In the second synthetic strategy, Au–$Fe_xO_y$ dumbbell nanocomposites could be synthesized by mixing all precursors in one pot, which will be decomposed upon heating to yield the nano-dumbbells. The precursors used in this strategy are virtually the same as the first strategy, with only minor synthetic modifications (Choi et al., 2008) However, despite a simpler synthetic procedure, the synthesized nano-dumbbells possess lower qualities in terms of their monodispersities, when compared to the nano-dumbbells synthesized via the first strategy. That is, core/satellite and aggregated composite structures would be obtained with a prolonged reaction time.

#### 2.2.1.1.5 Nano-flower structures

Nano-flowers could be regarded as any nanoparticle that resembles a flower-like structure with a core and multiple pedals. One of the Au–$Fe_xO_y$ nano-flower morphologies is the multiple dumbbell type. That is, each nano-flower is composed of one single Au core, surrounded by a few FexOy nanoparticles of similar size. The synthesis of such nano-flowers is similar to nano-dumbbells mentioned above, with altered stoichiometric ratio and reaction conditions. In brief, the synthesis involves decomposition of $Fe(CO)_5$ and its subsequent oxidation to yield Au@ $Fe_3O_4$nano-flowers, composed of $Fe_3O_4$nanoparticle pedals with an average size of 13.4 nm and a Au core of 8 nm (Xie et al., 2011). Generally speaking, this type of nano-flowers is actually derived from nano-dumbbells.

In a study performed by Grzybowski et al., it was discovered that different stoichiometric ratios of Au and Fe precursors will lead to a gradual change of morphology from dumbbells to flowers. When more Fe precursor was used relative to Au precursor, the formation of nano-flowers was preferred, and larger flower pedals were observed when the relative amount of Fe precursor increased (Figure. 2.4). Also, a prolonged reaction time would convert the synthesized nanoparticle from dumbbells to flowers gradually (Wei et al., 2008)

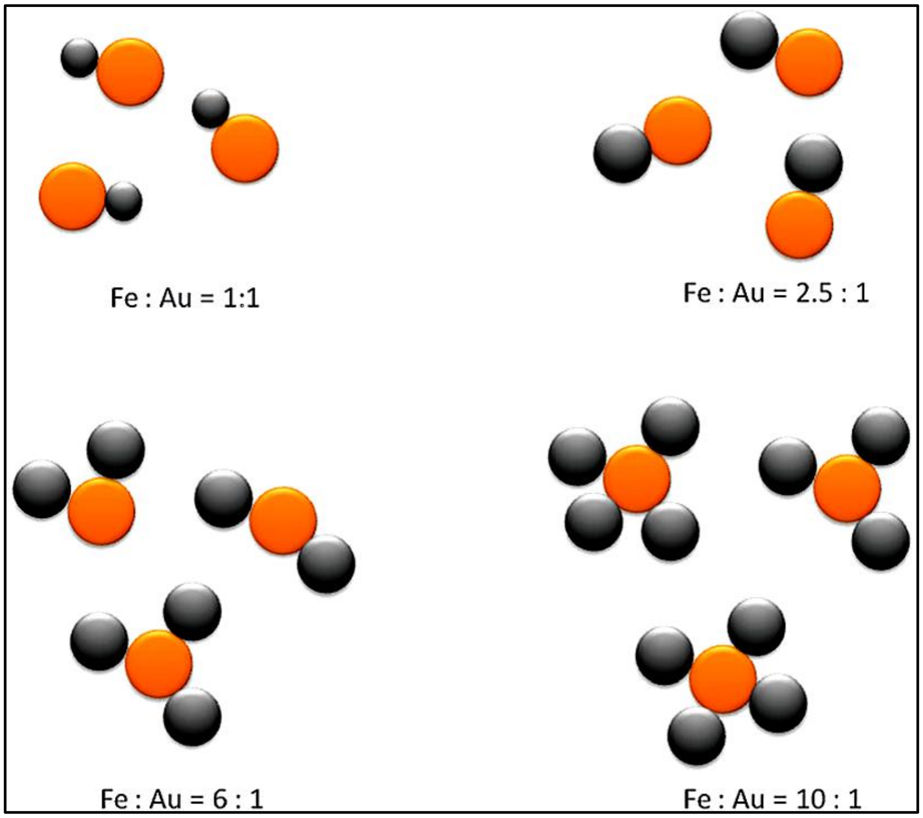

**Figure 2.4:** Schematic representation of the gradual change from Au-$Fe_xO_y$ nano-dumbbells to nano-flowers as the Fe:Au ratio increases. (Ken et al., 2012)

Another type of Au–$Fe_xO_y$ flower nanocomposites was reported by Feldman et al., which were synthesized by clustering from $Fe_3O_4$@Au core/shell nanoparticles. Pre-synthesized dextran-coated $Fe_3O_4$nanoparticles were dispersed in water and hydroxylamine. Au nanoparticles were deposited onto the $Fe_3O_4$core, by adding $HAuCl_4$ in a few aliquots, and then subsequently reduced by dextrose. A core/shell structure would be formed, and further deposition of metallic Au could cause clustering of the core/shell nanoparticles, yielding nano-flowers (nanoroses) with a range of sizes at 20–30 nm (Fieldman et al., 2009). Furthermore, by incorporating binding materials between $Fe_xO_y$ and Au nanoparticles, flower-like nanocomposites could also be obtained. Binding material such as aluminate (γ-AlOOH) has been reported recently. Silica-coated $Fe_3O_4$nanoparticles were modified with hierarchical aluminate sheets, followed by functionalization using 3-aminopropyltriethoxysilane (APTES) and self-assembly with citrated-coated Au nanoparticles (4 nm), yielding a flower-like nanocomposite structure having a size of around ~400 nm (Xuan et al., 2011).

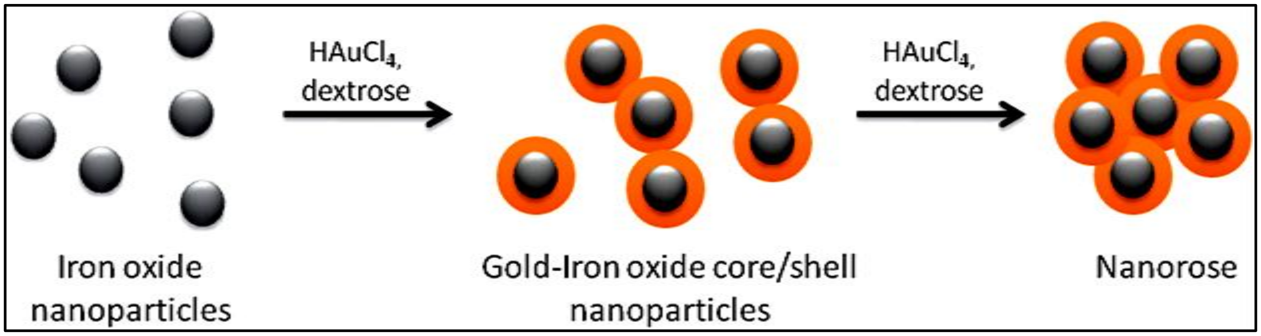

**Figure 2.5:** Formation mechanism of multi-core Au-$Fe_xO_y$ nanoroses structure (Ken et al., 2012).

### 2.2.1.2 Aggregates

Au–$Fe_xO_y$ aggregate composites possess random and polydispersed structures whereas the syntheses of these composites are sometimes simple, when compared to other well-defined, monodispersed Au–FexOy nanocomposites. In the synthesis of Au–$Fe_xO_y$ aggregates, there are generally two strategies. The first one is radiation-induced random aggregation, while the second strategy involves self-assembly of Au and $Fe_xO_y$ nanoparticles via a polymer wrap.

The radiation-induced random aggregation developed by Nakagawa et al. involves the simple mixing of polyvinyl alcohol (PVA), pre-synthesized $Fe_3O_4$nanoparticles and $HAuCl_4$ in an alcoholic solvent, followed by irradiation with a high dose of electron beam or gamma radiation (ca. 6 kGy). The synthesized aggregates are stabilized by PVA. In the second strategy, Stayton et al. reported that Au nanoparticles and $Fe_3O_4$nanoparticles could be randomly brought together by a polymer. Thermally responsive poly(N-isopropylacrylamide) (pNIPAAm), which served as the binding agent, was coated onto the Au and $Fe_3O_4$nanoparticles (Figure. 2.6). At a temperature higher than the lower critical solution temperature (LCST), the Au and $Fe_3O_4$nanoparticles would be aggregated together. When the temperature drops below the polymer's LCST, the aggregate components would be separated (Garcia et al. 2011).

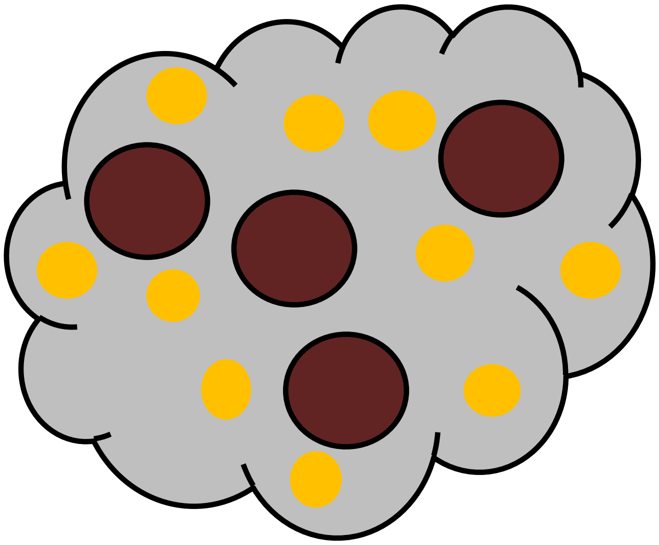

**Figure 2.6:** Schematic of aggregate formed from pNTPAAm coated Au and $Fe_3O_4$ nanoparticles.

### 2.2.2 Application of Composite Nanoparticles

In this section, selected applications of Au–$Fe_xO_y$ hybrid nanocomposite particles, which include magnetic resonance imaging, computed tomography, fluorescent optical imaging, magnetic-induced hyperthermia, photo-induced hyperthermia, gene delivery, DNA sensor, immunosensor, enzyme-based sensor, cell sorting, and catalysis, are discussed.

#### 2.2.2.1 Biomedical Imaging

Au–$Fe_xO_y$ hybrid nanocomposite particles are applied in both theranostic and diagnostic imaging purposes. With the advancement in biomedical application of Au–$Fe_xO_y$ hybrid nanocomposite particles are rapidly emerging, which include disease diagnosis at an early stage, monitoring and treatment of various diseases without hindering physiological condition. Magnetic resonance imaging or MRI is a noninvasive method for human in vivo imaging. Au-$Fe_xO_y$ composite nanoparticles are attractive materials for MRI process and these different shapes and sizes can have different magnetic properties which can be fine-tuned for better imaging results (Sun et al., 2008). These composite nanoparticles can also be used in computer tomography (CT) which is one of the most commonly used diagnostic tools in health centers. It measures the absorption of X-ray when it passes through the tissues. Due to the differentiations in X-ray attenuation of different tissues, the contrast image of anatomical structures can be produced. In principle, the degree of X-ray attenuation coefficient greatly depends on the atomic number and the electron density of the tissues. In the last decades, Au nanoparticles have been proposed as CT contrast agents due to their high electron density and high atomic number (Kim et al., 2007). However, the CT imaging technique is not sufficient to perform diagnosis accurately due to its inherent weakness. Recently, a multimodal imaging contrast agent is introduced by $Fe_3O_4$@Au core/shell nanocomposites (Jeong et al., 2011). The nanocomposite showed a high CT attenuation due to the presence of Au layers but had a relatively lower T2 signal intensity in MRI than normal SPIONs due to the embedded $Fe_3O_4$ core. Another application of these composite nanoparticles is in fluorescent optical imaging (FOI). FOI is a technology that measures light produced from fluorescent-labeled biological or chemical moieties. It is another noninvasive method for visualization of biological phenomena inside living animals with bio-engineered fluorescent proteins, dyes or conjugates into cells. Recently, with the surface functionalization platform of the Au surface of Au–$Fe_xO_y$ nanocomposites, fluorescent probes can be conjugated to them via a Au–S bond, to develop a multi-modal MRI-FOI contrast agent.83 In addition, some studies reported that Au nanoparticles exhibit remarkable optical properties due to excitation of their surface plasmons by incident light, resulting in a significant enhancement of the electromagnetic field at the nanoparticle surface (Bardhan et al., 2009). Based on this enhanced fluorescence effect, a multi-modal imaging contrast agent, which is based on $Fe_3O_4$@Au@$SiO_2$-ICG cluster/shell/shell nanocomposite, has been prepared. The nanocomposite could dramatically enhance the fluorescence intensity of indocyanine green (ICG), rendering them useful fluorescent contrast agents.

#### 2.2.2.2 Theranostic Hyperthermia

Hyperthermia is referred to the heating of superficial tumor to cure the illness. The location of the hyperthermia can be within a specific region or an entire body region. Cell death can occur when the temperature of the region increases above 42˚C whereas apoptosis will begin to take place from 41 to 47˚C while necrosis will begin to take place upon 50˚C (Curleya et al., 2010). For apoptosis, pro-apoptosis proteins would induce caspase-9 which will lead to cell death, while necrosis will denature the protein immediately due to the boiling of the cells. Hyperthermia is achieved by using radio-frequency, microwave and laser which involve the introduction of a probe in to the body region. In recent times Au-$Fe_xO_y$ composite nanoparticles are applied in hyperthermia in magnetic-induced hyperthermia and in photo-induced hyperthermia.

#### 2.2.2.3 Other Major Application

Au-$Fe_xO_y$ composite nanoparticles are applied in targeted drug delivery, where the region of infection or the diseased part is first detected using the imaging property of the composite nanoparticles and then the drug attached to the Au-$Fe_xO_y$ composite nanoparticles by surface modification works on the infected region. They can also act as a gene delivery system as DNA or RNA can be easily attached to the Au-$Fe_xO_y$ composite nanoparticles surface. Au-$Fe_xO_y$ composite nanoparticles which are functionalized with thiolated biomolecules can also act as DNA based biosensor, enzyme based sensor or immunosensor. These sensory properties of the Au-$Fe_xO_y$ composite nanoparticles can be further modified to act as a cell sorting and bio-separation agent. Another main application of Au-$Fe_xO_y$ composite nanoparticles is catalysis. In the last decade, Au nanoparticles have played an important role in several catalytic processes including hydrogenation, low-temperature carbon monoxide oxidation, alcohol oxidation, alkene oxidation, reductive catalysis of chloro- or nitrohydrocarbons and organic synthesis. Recently, Au–$Fe_xO_y$ nanocomposites and their derivatives were introduced to successfully demonstrate the catalytic effect towards carbon monoxide oxidation (Hung et al., 2010), synthesis of hydrogen peroxide (Edwards et al., 2005), reduction of nitrophenols (Lin & Doong, 2011) and reduction of hydrogen peroxide (Lee et al., 2010).

### 2.3 Biogenesis of Nanoparticles

In recent times biological routes of nanoparticles synthesis are more preferred over the chemical routes of synthesis as more and more nanoparticles are being applied in theranostic and diagnostic purposed. Nanoparticles synthesized by biological routes are cytocompatible and are often stabilized or capped by a biodegradable material. The biogenesis of nanoparticles can be sub-divided into five categories by the type of biomaterials used namely: plant, bacteria, fungi, algae, actinomycetes and in two categories by intracellular or extracellular type of synthesis. Biogenesis of nanoparticles and the synthesis approach of nanoparticles by different biomaterials are discussed below.

### 2.3.1 Classification of Biogenesis Approaches

#### 2.3.1.1 Plant Mediated Biogenesis of Nanoparticles

Plant mediated synthesis of nanoparticle is comparable to chemical and physical methods of nanoparticle synthesis in the term of shape and size of particle formed (Parsons et al., 2007). Plant mediated synthesis are simpler and more cost-effective in contrast to microorganism mediated synthesis of nanoparticles (Banker et al., 2010). Plant mediated biogenesis of nanoparticles can be performed in aqueous medium than solvents, thus making the process environmentally benign and cost effective. Plant mediated biogenesis can occur on either live plant or plant biomass like plant derived biomolecules or plant extract.

Hyperaccumulators are plant or organism which can accumulate a material in a concentration of more than 100 times of the normal concentration of accumulation. Plant and other organism due to stress or strain had to change their genetic map over many generations to survive in an adverse atmosphere. The accumulators or hyperaccumulators such arose to deal with contaminated soil, or shortage of nutrients. Sometime the plants or organisms take up the material present in atmosphere in high condition and store it for later usage or excretion. Some plants have evolved over time to endure high concentration of certain metal like antimony, arsenic, cadmium, copper, nickel, selenium, thallium, manganese and zinc depending on the ecological condition. These plants accumulate metal in a higher concentration than the surrounding ecological system. Presences of these hyper accumulating plants have long been noted in and around mines, waste land, sewerage lines etc. The most modern definition describes hyperaccumulator as a plant which can accumulate metal 100 times greater than the non-accumulating plant.

The first documented presence was a perennial shrub, named *Alyssum bertolinii* which had a nickel content of 0.79% by mass in dried leaves, whereas the soil contained only 0.42% nickel. Hyperaccumulator plant *Berkheya coddii* was used in the late 1990s in Rustenberg, South Africa to decontaminate land near the Rustenberg smelter. The nickel uptake was 2-3% by mass of the dried plant. Ashes of dried plants containing about 15% by mass were added to the bulk metal ore and returned to smelter. Over time hyperaccumulators have been used for phytoremediation and phytomining. It is well known that the ability of plants to uptake gold has made them natural bio-indicator of gold deposits. Several theories exist regarding the transformation of metallic salt to nanoparticle. One hypothesis is that nanoparticles may be formed on the roots and then be transported in the plant body (Gardea-Torresdey et al., 2003; Sharma et al., 2007). Another hypothesis is that the metallic salt in ionic form is transported to the plant body through root vascular system and then the metallic salt is reduced to nanoparticles intracellularly by biomolecules (Gardea-Torresdey et el., 2005a).

Plant biomass includes plant leaf, root, shoot and usually an extract from the plant parts are used for synthesizing nanoparticles. In a plant biomass mediated biogenesis of nanoparticle the inactivated plant material acts as three agents simultaneously such as reducing agent, stabilizing agent and capping agent. There are three distinctive reaction regimens during the biogenesis mechanism: a short induction period, a growth phase and a termination period. Metallic ions interact with biomass through ionic bonding with bioreducing agents such as flavonoids, terpenoids, organic acids, reducing sugars, proteins and enzymes. A the reducing rate of bioreducing agents are slow than the metallic seed it leads to a slower rate of growth of nanoparticle resulting in formation of small particles. Some nanoparticles are capped with biomolecules which provide them with extra solubility or stability. This adsorption of biomolecules on the surface of metallic nanoparticle can be attributed to the presence of π-electrons and carbonyl groups in their molecular structures. Diverse natures of biomolecules are responsible for the synthesis of nanoparticles such as terpenoids, flavonoids, polysaccharides, proteins and alkaloids. These functional groups act as both the potential reducing agent and the stabilizing agent.

The biogenesis of nanoparticles with plant extract has recently been extended in the field of composite nanoparticles. The extract of red and green cabbage was used to obtain silver, anisotropic gold and composite silver-gold nanoparticles. Simultaneous reduction of both silver and gold precursors leads to formation of composite type particles (Jacob, Mukherjee, & Kapoor, 2012). Indian rosewood or *Dalbergia sissoo* was used to obtain both monometallic and composite gold-silver composite nanoparticles (Roy et al., 2012). Neem or *Azadirachta indica* is a plant with several medicinal and beneficial properties and the leaf of this plant has been used for centuries for therapeutic and other purposes. A mixture of gold and silver precursor solution in 1:1 ratio was reduced by Neem leaf broth to form a composite $Au_{core}$-$Ag_{shell}$ structure (Shankar et al., 2004). *Cacumen platycladi* leaf extract was used to synthesize Au-Ag and Au-Pd composite composite nanoparticles (Zhang et al., 2013), (Zhan et al., 2011). An aqueous suspension of powdered milled alfalfa (*Medicago sativa*) was used to obtain composite Ti/Ni nanoparticles in a pH dependent process (P.S. Schabes-Retchkiman et al.. 2006). Another study showed the usage of Persimmon *Diopyros kaki* or leaf extract for synthesis of composite Au-Ag nanoparticles (Kim and Song, 2008). *Piper bettle L.* from *Piperaceae* leaf extract assists in the formation of silver-protein core-shell nanoparticle (Pathipati and Pala, 2011). Composite Au-Ag nanoparticles were biogenesised upon reaction with *Anacardium occidentale* aqueous leaf extract (Philip et al., 2011).

### 2.3.1.2 Microorganism Mediated Biogenesis of Nanoparticles

Microbial synthesis of nanoparticle can be intracellular or extracellular. Normally most metals show toxic reactivity towards microbes varying from different genre. However there are some bacteria which reduce the metal to counteract the toxic effect. This process can be generally termed as metal specific resistive toxicity and reductivity. Bacteria from totally different genre can reduce metal distantly linked to its nutrition. Bacteria groups which are linked to sulfur cycle, nitrogen cycle and other environmental cycle are mostly responsible from this resistive toxicity. Sulfur bacteria can reduce material by sulfur reductase enzymes, whereas, bacteria which are linked to nitrogen cycle produce nitrogen reductase enzyme which in turn forms nanoparticle. Extracellular synthesis occurs when metal is reduced by enzymes or biological agent secreted by bacteria and intracellular biogenesis occur when metal I taken up by bacteria by macro-phaging and then reduced to nanoparticulate form and then either excreted or stored in vacuoles for further use or disposal.

Fungi are found to be more advantageous compared to other microorganisms in many ways. Fungal mycelial mesh can withstand flow pressure and agitation and other conditions in bioreactors or other chambers compared to plant materials and bacteria. These are fastidious to grow and easy to handle and easy for fabrication. The extracellular secretions of reductive proteins are more and can be easily handled in downstream processing. And when, nanoparticles are deposited extracellularly without any unnecessary cellular components, the as synthesized nanoparticles can be used directly. Two types of synthesis pathways exist intracellular and extracellular. The nanoparticles synthesized intracellularly are smaller in dimension than the extracellular ones, which may be due to nucleating in a small space inside the organism. But the intracellularly synthesized nanoparticles are capped or attached with unnecessary biomolecules which render them unable to be used directly and separation and purification from an intracellular system is quite problematic. These types of problems do not arise in extracellular synthesis where the nanoparticle is devoid of any unwanted biomolecule attachment due to the enormous secretory reducing component of fungi and their capping effect. Other microorganisms such as actinomycetes, algae and yeast share the same synthesis approach for production of nanoparticles.

Similar mechanism such as hyper accumulating plants can be found in microorganisms which use different material as a chief source of nutrients like sulfur reducing bacteria, magnetotactic bacteria which take up sulfur or iron from surroundings and then produces elemental sulfur or sulfur material and in case of iron by oxidizing ferrous ions to ferric oxide and forming brown colored slime. These kinds of bacterias are proteobacteria and are normally facultative anaerobe. *Pedomicrobium sp*. hyper accumulates gold (Mann, 1992), iron (Fe (III) reducing bacteria *Geobacter ferrireducens* and *Shewanella algae*, reduce and precipitate gold in periplasmic space and on bacterial surfaces (Kashefi et al. 2001; Konishi et al., 2007), *Plectonema boryanum* UTEX485 accumulates gold in membrane vesicles (Lengke et al., 2006), *Stenoprophomonas maltophilia* SELTE02 accumulates selenium (Se) and reduces it in cell cytoplasm (Gregorio et al., 2005).

There have been reports of numerous documentation where a microorganism has been used for fabricating single nanoparticles. In modern times these microorganisms are also also being used for synthesis of composite or core/shell nanoparticles. *Neurospora crassa* is a non-pathogenic, filamentous fungus which is used as a model organism in biological field. Commonly known as red bread mould, *Neurospora crassa* produced silver, gold and composite gold-silver composite nanoparticles intracellularly when incubated with $AgNO_3$ and $HAuCl_4$ for 24 hour (Castro-Longoria et al. 2011). Yeast or *Saccharomyces cerevisiae* forms Au-Ag composite type nanoparticle extracellularly (D.Zhang et al., 2010). Another extracellular synthesis of composite Au-Ag nanoparticle was reported by Daizy Philip (Philip, 2009) by edible mushroom extract. Fungus *Fusarium semitectum* was utilized for extracellular synthesis of Au-Ag composite type bitmetallic nanoparticle in an aqueous medium (Prabhakar et al.2008). In a hybrid biochemical synthesis route *Eserichia coli* aides in the synthesis of $Au_{core}$-$Pd_{shell}$ nanoparticles (Deplanche et al. 2012). *Spirulina platensis* is gaining more attention everyday as a manufacturing site of single cell protein used in many nutritional and pharmaceutical industries. *S.plantesis* has been also used for the biogenesis of $Au_{core}$-$Ag_{shell}$ nanoparticles (Govindaraju et al., 2008).

### 2.3.1.3 Biomolecules mediated Biogenesis of Nanoparticles

In addition to different plant and microbial organisms several biological molecule such as carbohydrates, proteins, enzymes etc. have been used for biogenesis of nanoparticle. Glucose and starch are two elemental form of carbohydrates found in the environment. Glucose is a mild reducing agent which can be activated by mild heating or by a basic catalyst. Glucose and starch were used in different stoichiometric ratios for starch-protected synthesis of metallic silver (Ag), gold (Au) and gold-silver (Au-Ag) composite. Starch has also been used as only stabilizing agent whereas ascorbic acid is the reducing agent in a microwave assisted process for biogenesis of silver-copper composite nanoparticles. In this study Valodkar et al. (Valodkar et al., 2011). NADPH or β-nicotinamide adenine dinucleotide 2'-phosphate is an important bio-reducing agent in cellular metabolism as a hydrogen donor. NADPH was utilized as a slow reducing agent for synthesizing Au-Ag composite composite nanoparticle. Silver-nickel core-shell nanoparticle was synthesized by using skin collagen fiber (SCF) as a bio-template for the reaction and bayberry tannin as a reducing agent (Liao et al. 2012). Tyrosine, an amino acid has a pH-dependent reducing capability, which arises due to ionization of the phenolic group of tyrosine at high pH, which after electron transfer transforms to quinone. A chemically reduced Au seed capped with tyrosine was used for core-shell nanoparticle formation with a silver shell. Silver precursor was separately reduced to silver nanoparticles by a pH dependent reduction mechanism of tyrosine (Sastry et al., 2004). Au-Ag composite nanoparticle was synthesized by utilizing α-amylase an enzyme which hydrolyses large carbohydrate molecules such as starch and glycogen, in place of a reducing agent( Faramarzi et al., 2011).

## 2.4 Concluding Remarks

This chapter seeks to emphasize how the research field of Au-$Fe_xO_y$ composite nanoparticles has been diversifying over the past two decades. The biomedical application of Au-FexOy composite nanoparticles has directed the research into the field of biological synthesis of nanoparticles. Biogenesis of nanoparticles contributes to the cytocompatibility of the Au-$Fe_xO_y$ composite nanoparticles a main point of concern for bio-applicability of such nanoparticles. Different structural form of the Au-$Fe_xO_y$ composite nanoparticles are also discussed in this chapter. The modern application of the Au-$Fe_xO_y$ composite nanoparticles shows how important they are for developing modern technologies for theranostic and diagnostic purposes. Different biogenesis methods has been discussed for synthesis or composite or core/shell nanoparticles. Throughout this literature survey we concentrated only on Au-$Fe_xO_y$ composite nanoparticles' structural classification and synthesis approaches, and synthesis approaches of composite nanoparticles by biological methods. Brief review of gold and iron oxide synthesis methods are not included in this chapter and are mentioned in the respective chapters later in this study.

## 2.5 Objectives of the Work

The review literatures presented in this chapter confirms that most Au-$Fe_xO_y$ composite nanoparticles are synthesized in wet chemical methods in presence of external surfactant, dispersing medium, co-surfactant and a separate reducing agent is used. Literatures show that the Au-$Fe_xO_y$ composite nanoparticles are in strong demand for their multi-disciplinary applications in biomedical imaging, drug delivery, bio-separation, bio-sensor, catalysis etc. Other literature survey shows that biological based systems are capable of synthesizing composite or core/shell nanoparticles. So, the overall objective of the work is to develop easy aqueous based one-pot synthesis method for Au-$Fe_xO_y$ composite nanoparticles by a biological system.

The primary objectives of the research work are as follows:

(i) Synthesis of gold Au nanoparticles in a one-pot aqueous green route synthesis method.

(ii) Synthesis of iron oxide ($Fe_xO_y$) nanoparticle in a one-pot aqueous green route synthesis method.

(iii) Synthesis of gold-iron oxide (Au-$Fe_xO_y$) composite nanoparticle in a one-pot aqueous green route synthesis method.

# Chapter 3

# Synthesis of Gold Nanoparticles Using Tea Extract

## 3.1 Introduction

Gold nanoparticles (Au NPs) are significant nanoscale materials that have been under extensive observation for quite a long time as they exhibit significantly new and enhanced properties compared to bulk phase. Different approaches involved in the preparation of noble metals like gold has attracted prominence owing to its noteworthy size-dependent optical and electronic properties. Gold nanoparticles are exclusive due to their tunable Surface Plasmon Resonance (SPR). They are applied in bio-labeling (Lin et. al., 2009), biosensor devices for the detection of bacteria and viruses (Xia et. al., 2007), biomedical science including drug delivery (Niemeyer, 2001), tissue or tumor imaging and cellular optical imaging (Basha et. al., 2010, Kisailus et. al., 2005, Song et. al., 2010, Edelstein & Cammarat, 1966), hyperthermia and sensitive bio detection of DNA and proteins. The plasmonic resonance peak of gold nanoparticles can be further shifted to NIR region by fine-tuning the morphologies and vicinities of the particles (Mulvaney, 1996).

Due to recent awareness of application of nanoparticles in diagnostic and theranostic practices, it has been determined that gold nanoparticles are biocompatible, inert (Horisberger et al., 1977), bind readily to a large range of biomolecules such as proteins or enzymes (Niemeyer et. al., 2001, Keating et.al., 1998), DNA (Alivisatos et. al., 1996), amino acids (Sastry et. al., 2004, Sastry et. al., 2003) and expose large surface area for the immobilization of such biomolecules and environmentally friendly chemicals. Synthesis of gold nanoparticles has many different approaches: including traditional citrate reduction (Brust et. al., 1994), the widely employed Brust-Schiffrin method of two-phase synthesis with thiol stabilization (Slot & Geuze, 1981), seeding growth using ascorbic acid (4), and several thermal and photochemical techniques using thiols (Brust et. al., 1994), amines (Slot & Geuze, 1981), micelles (Maier et. al., 2003), dendrimers (Elghanian et. al., 1997), polymers (Liu, Xu & Kaifer, 1998), biomolecules (Andres et. al., 1996), and ionic liquid (Wisian-Neilson & Neilson, 1989) as protective agents to help in their stabilization in aqueous, organic and thin film media (Wisian-Neilson & Garcia-Alonso, 1993, Alvarez et. al., 1997). But there is a developing interest to cultivate clean, nontoxic, and ecologically benign synthesis technologies. Biogenesis of metal nanoparticles using natural products is an emergent area for nanoscience research. As natural environment has a diverse source of plants, extracts of plants, marine organisms, and microorganisms, we have a vast range of biological based systems to choose from for synthesis of nanoparticles. In the last few years there have been several reports on the usage of natural materials for synthesis of gold nanoparticles ranging from plants, algae, fungi, bacteria, yeast etc. both intracellularly and extracellularly.

Several plant extracts have been used to synthesize gold nanoparticles, but recently the trend has turned towards usage of plant extracts with more beneficial properties. Tea has been associated with plethora of health benefits (Amin & Buratovich, 2007, Friedman, 2007) from bygone era. Tea drinking has shown beneficial effects of cardiovascular diseases, reducing the risk of cancer, enhancing immune function and aiding dental health. Tea contains high level of antioxidant polyphenols, including flavonoids, and catechins, all of which scavenges harmful free radicals from body and boost the immune function. Tea with its myriad ranges of polyphenolic flavonoids, have a diverse range of reduction potential, thus can be used as a reducing agent in a aqueous medium for producing gold nanoparticles. In this study, commercially available tea leaf extract used to synthesize gold nanoparticles in an aqueous system without the presence of any surfactant or dispersing medium. The main objective of this chapter is to study the synthesis of gold nanoparticles in a aqueous medium using tea extract and to characterize the as synthesized gold nanoparticles to confirm the formation of the gold nanoparticles.

## 3.2 Experimental Section

### 3.2.1 Materials

The required chemicals were purchased from the following sources: chloroauric acid ($HAuCl_4$, $xH_2O$) from Sigma-Aldrich with 99% assay and commercially available tea leaf (Red Label) from Tata India Ltd., with 99% purity. Ultrapure water of 18.2 MΩ cm resistivity and 6.4-6.5 pH was used for all the experiments. The constant temperature of 25±0.5˚C was maintained throughout the experiments. The gold precursor was used as received but the tea leaf extract was prepared in ultrapure water explained in detail in the next section.

### 3.2.2 Synthesis Techniques

#### 3.2.2.1 Preparation of Tea leaf extract

Tea leaves from commercially available brand Red Label (Tata India Ltd., 99% purity) was purchased and 2 grams of tea leaf was mixed in 100 ml of ultrapure water (2% w/v), and then heated at 100˚C for 20 min in a hot water bath. The residue was separated by filtration first through Whatman No. 42 filter paper and secondly through a filter of 0.45µm pore size. Finally the leaf extract was centrifuged at 20,000 rpm (Sigma, Model No. 3-30K, Germany) for 15 minutes to remove any ultrafine suspended particles. The pH of the tea extract was determined at almost neutral ~6.5.

#### 3.2.2.1 Synthesis of Nanoparticles

Gold nanoparticles were prepared from aqueous $HAuCl_4$ solution (0.1-0.0001 mM) as a precursor, and using the as prepared tea extract as a reducing agent in aqueous medium. A constant ambient temperature of 25˚C was maintained throughout the process, where the $HAuCl_4$ solution was stirred continuously and 10 µl of tea extract was added to the solution. Within 15 min of addition of tea extract, the color of the solution changed from pale yellow to pale pink, ruby red, and deep purple depending on the precursor concentration respectively, indicating the formation of gold nanoparticles. The resulting solution was sonicated by using a probe type sonicator using 260 watt for 10 min. After a waiting period of 30 minutes the solution containing the particle were centrifuged at 25,000 rpm for 15 minutes, and washed with double distilled water thrice.

### 3.2.3 Particle Characterization

Particle size measurement was carried out by dynamic light scattering (DLS) using Malvern Zeta Size Analyzer, U.K. (Nano ZS). The particles were characterized by UV-vis NIR Spectroscopy (Shimzadu-3600), FT-IR Spectroscopy (Thermo-Fischer-Nicolet iS10) ), X-ray Diffraction (XRD) (Philips, Pw, 1830 HT) and Energy-dispersive X-ray diffraction spectroscopy (EDX) attached with the field emission scanning electron microscope (FESEM) (Nova Nano SEM/ FEI) used to observe the size and shape of the particles.

## 3.3 Results and Discussion

### 3.3.1 Characterization of Particles by UV-vis Spectroscopy

UV-vis spectroscopy was used for characterization of the nanoparticles formed using tea extract upon the different concentration of $HAuCl_4$ solution. Absorption measurements of the gold nanoparticles show that the plasmon resonance wavelength $\lambda_{max}$ of the as synthesized nanoparticles at around 532 nm wavelength. The absorption spectra of these particles are shown in Figure 3.1. The absorption peaks shifts to longer wavelength (red shift) when the gold precursor concentration increases, indicating that the particle size increases but at the same time the particle size distribution becomes much wider (as shown in Figure 3.5) with increasing $AuCl_4^-$ concentration. The inset of photograph (Figure 3.1) shows the physical appearance of the different concentrations of gold reactant. In the presence of very dilute $AuCl_4^-$ (0.0001 mM) solution the physical appearance of the suspension is pale pink.

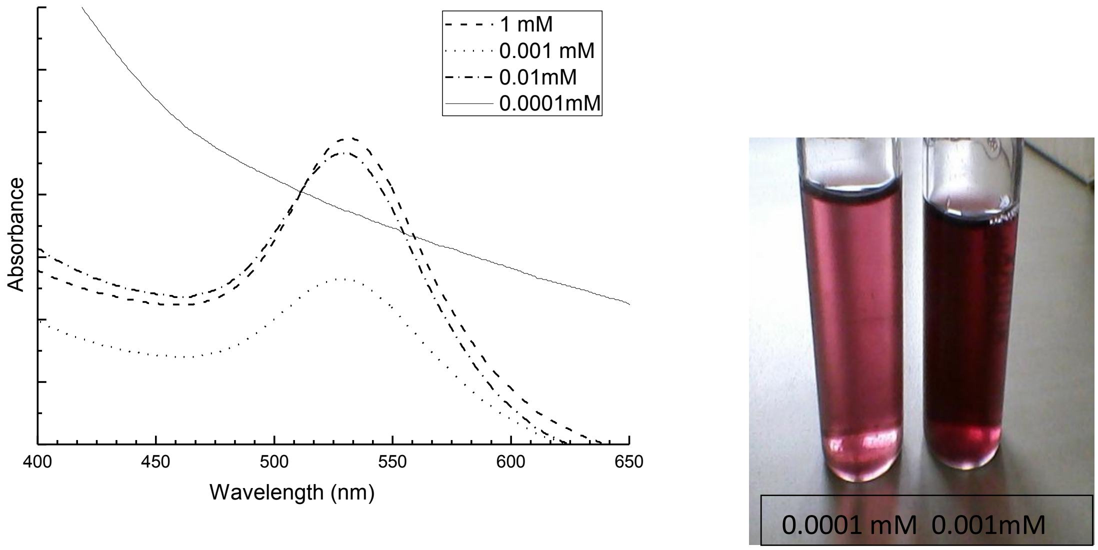

**Figure 3.1:** Surface plasmon absorbance of spherical Au nanoparticles with increasing $AuCl_4^-$ solution concentration and the inset Figure shows the physical appearance of the respective solution with 0.0001 mM and 0.001 mM concentration of $HAuCl_4$ solution.

When the concentration of the gold solution increases, at the outset the color of the suspension is purple red, but when the concentration of $AuCl_4^-$ solution was increased further the color changes to ruby red, which is an indication of increasing particle size. When the concentration is 1 mM the appearance of the suspension becomes purple. In the Figure 3.1 the peak position at 0.001 mM $AuCl_4^-$ solution is 532 nm, whereas this peak shifted to 540 nm at 0.1 mM $AuCl_4^-$ solution concentration. The absorption peak intensity increases with increasing reactant concentrations, but in contrast the peak position does not differ significantly from 532 to 540 nm, that is because of the less variation in particle size with increasing concentration. Both the absorbance and peak shift for each solution exhibits three similar steps, a short lag phase where no color change in appearance occurs, after that comes the growth phase where a rapid change in physical appearance occurs indicating formation of gold nanoparticles, and a termination or saturation period where there is no further change in appearance. These three steps confirm with the three basic steps of biogenesis of nanoparticles as discussed before.

### 3.3.2 Characterization of Particles by FT-IR Spectroscopy

FT-IR characterization was done to get an idea about the functional groups present in the tea extract and the role of those groups in formation of the gold nanoparticles. The FT-IR spectra of the fresh tea extract before and after reduction of $AuCl_4^-$ solution are shown in Figure 3.2. The absorption bands in Figure 3.2(a) are observed in the region of 1000-1800 cm$^{-1}$ are 1683, 1623, 1362, 1213 and 1150 cm$^{-1}$. The absorption bands corresponds to different group frequency region, such as the absorption bands at 1683, 1623, 1362, 1213 cm$^{-1}$ are associated with the stretching vibrations of the –C=C–C=O and –C=C– in ring aromatic groups, –C–C– in ring aromatic group, C–O stretch of esters and ethers groups and C–O stretch of polyols groups respectively. In particular the 1213 cm$^{-1}$ band arises most probably from the C–O group of polyols such as hydroxyflavones and catechins, which are the main groups of functional material in tea extract. After the reduction of the $AuCl_4^-$ solution the predominant peaks disappear in the Figure 3.2(b). This may be due to the involvement of the functional groups in the bioreduction of the gold nanoparticles, whereby they themselves get oxidized to α, β-unsaturated carbonyl groups leading to a broad peak at 1646 cm$^{-1}$. There may be a probable mechanism of reduction which is explained later in the chapter.

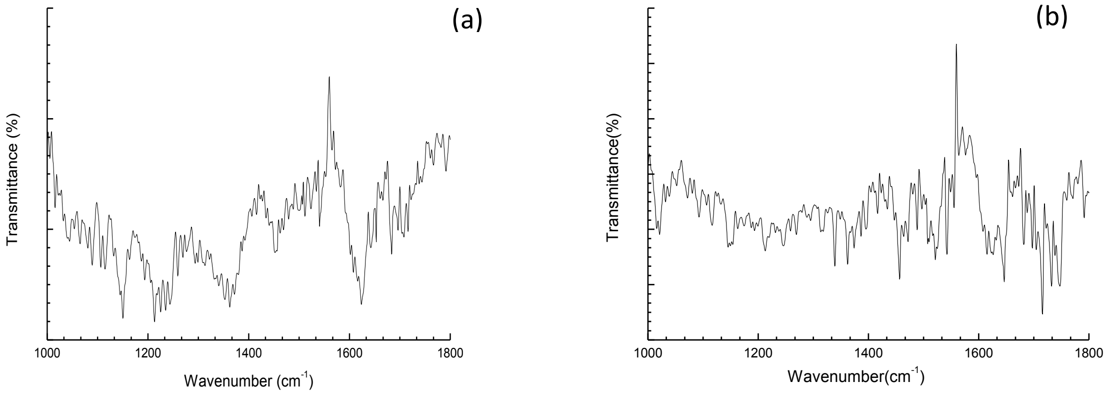

**Figure 3.2:** FT-IR images of (a) Tea extract, (b) Au NPs synthesized using tea extract.

### 3.3.3 Characterization of Particles by XRD

Gold nanoparticles synthesized by tea extract were characterized by X-ray diffraction analysis (XRD) and the Figure 3.3 shows the XRD pattern of those particles. Scans were performed over a 2-theta ranging from 30 to 80° with a step of 0.02° and a one second count time at each step. The XRD pattern of the Au nanoparticles matched with the cubic Au structure (02-1095 from JCPDS PDF number) with d-spacing of 0.2356 nm. The pattern visibly shows the main peaks at (2θ) 38.27°, 44.60°, 64.68° and 77.55°, which respectively corresponds to (111), (200), (220) and (311) planes. The pattern also shows that the (111) is the major plane with the majority of the particles showing face centered cubic (fcc) structure.

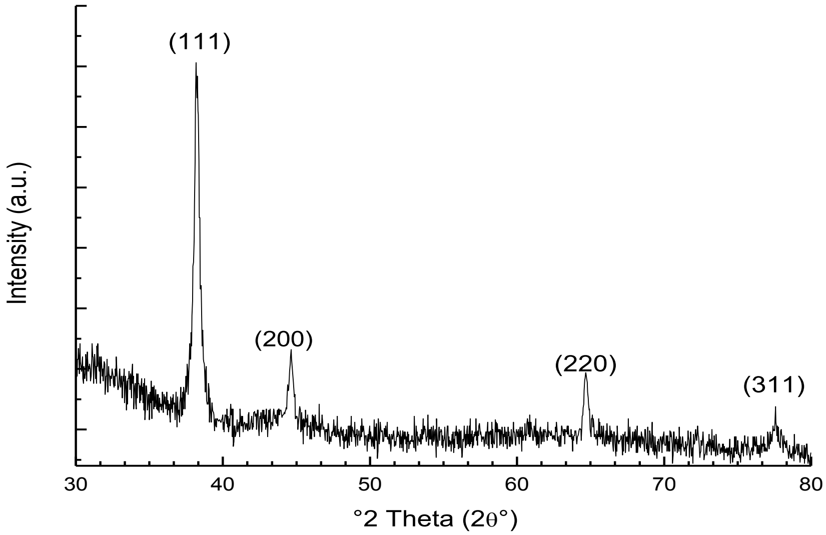

**Figure 3.3:** XRD pattern of Au nanoparticles as synthesized using tea extract.

### 3.3.4 Characterization of Particle Size and Morphology

The physical properties of the gold nanoparticles generated using tea extract were determined by field emission scanning electron microscopy (FESEM) and dynamic light scattering (DLS) techniques. The FESEM measurement of the Au nanoparticles synthesized from the AuCl4- (0.001mM) concentration solution using tea leaves show that the particles are spherical in shape within the size range of 10-60 nm and with an average size of ~30 nm. The particle size distribution from the FESEM data (Figure 3.4(a)) shows that the particles are well dispersed and close to the data (Figure 3.4 (b)) measured by the dynamic light scattering (DLS) method of size measurements. The variation in the size of the gold nanoparticles may be attributed to the presence of the tea phytochemicals namely catechins, theaflavins and thearibigins etc. capped to the surface of the gold nanoparticles. Additionally the FESEM analysis of the nanoparticles coupled with the EDX spectrum data (Figure 3.4 (c)) confirms about the gold nanoparticles.

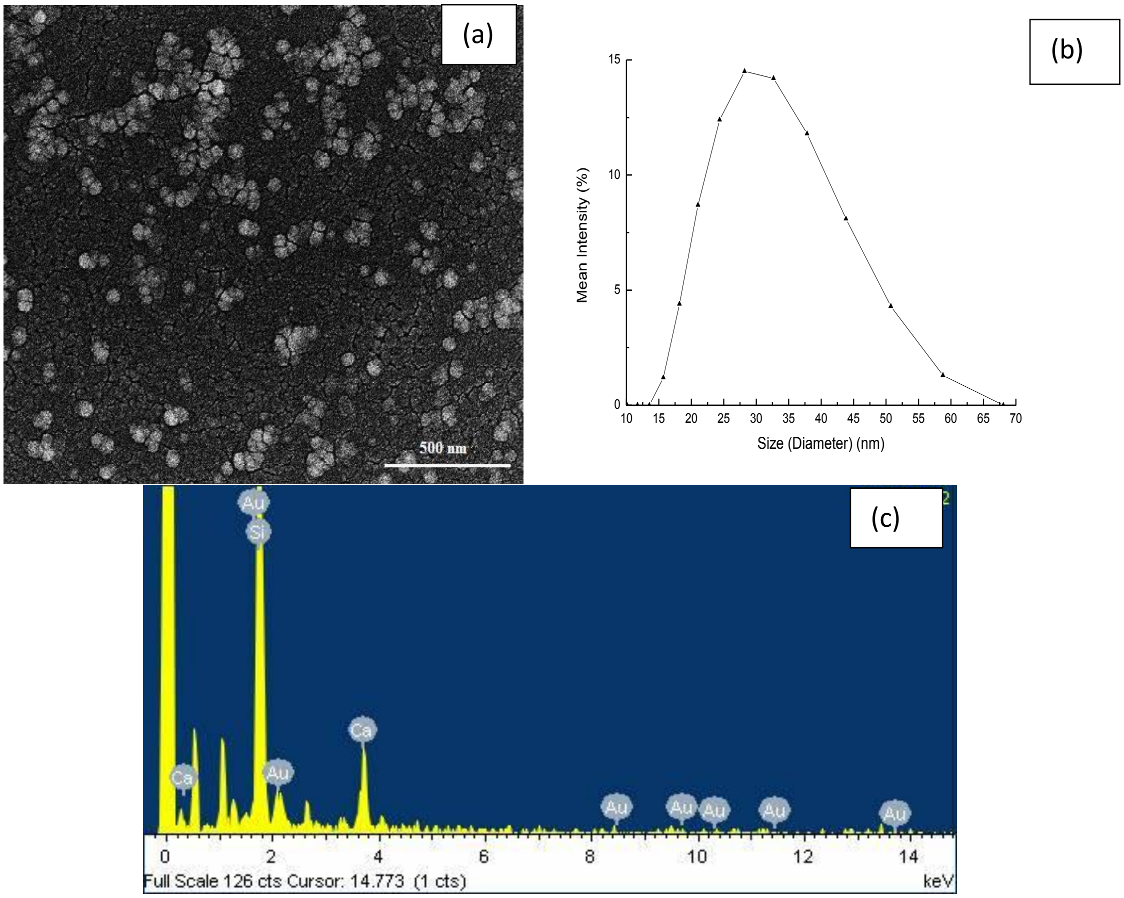

**Figure 3.4:** FESEM image (a), DLS data (b) and EDX analysis (c) of Au nanoparticles synthesized using tea extract.

### 3.3.5 Probable Mechanism of Nanoparticle Formation

As discussed earlier the probable mechanistic steps for the formation of gold nanoparticles involve a huge role by the tea phytochemicals. The aqueous tea extract can be broadly classified into two groups: catechins and theaflavins. Therefore water soluble extract of tea may possibly play a positive role in the overall reduction reactions of $HAuCl_4$. The roles of commercially available phytochemicals of tea in synthesis of gold nanoparticles have been previously mentioned (Nune et. al., 2009) The different commercially available catechins such as catechin, epicatechin, epicatechin gallate, catechin gallate, epigallocatechin, and epigallocatechin gallate were used for reduction of gold precursors and they showed excellent reducing and stabilization effect. Among the catechin group epigallocatechin gallate (EGCG) showed the most stabilization effect while epicatechin showed the least, but both lack the ability to effectively coat the nanoparticles to prevent from agglomeration. The other group of tea phytochemicals, theaflavins possesses both the strong reducing and stabilization influence. The combined effects of the catechins and theaflavins groups of phytochemicals reduce the $HAuCl_4$ solution and act as both the stabilizer and the dispersing media for well dispersed spherical gold nanoparticles. As brought up before that the metal ions may probably get reduced by the polyols ions of the tea phytochemicals whereas they themselves get reduced to α, β-unsaturated carbonyl groups. The plausible schematic of the process is illustrated in the Figure 3.5 below.

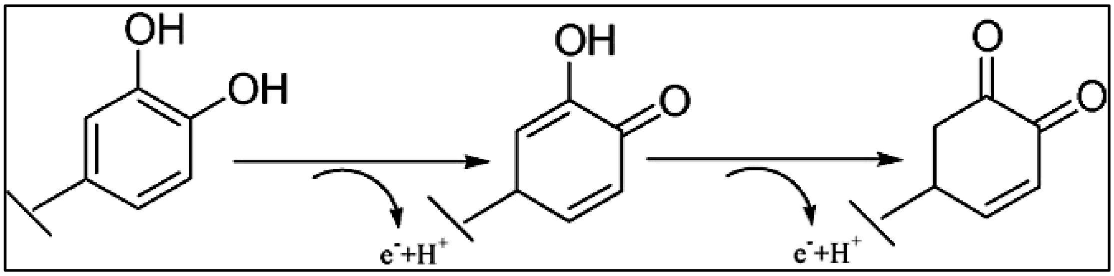

**Figure 3.5:** Schematic illustration of oxidation of polyol group by metal ions to α, β-unsaturated carbonyl groups.

The suppression of the absorption spectra of the polyol group (Figure 3.2) after the reduction of the $AuCl_4^-$ solution by tea extract, also hints at the involvement of the polyol group in the reduction and stabilization of gold nanoparticles. The reduction potential of the catechin and flavonoid groups of the tea extract falls in the range between 0.3 to 0.8 V and the reduction potential values of $AuCl_4^-$ ion or $Au^{3+}$ ion are 1.002 V and 1.52 V for a one step conversion to Au nanoparticles. For a two-step process the standard reduction potentials of both $AuCl_4^-$ ion and $Au^{3+}$ ion are respectively as below.

$$Au^{3+} \xrightarrow{1.36\ V} Au^{+} \xrightarrow{1.83\ V} Au$$

$$AuCl_4^- \xrightarrow{0.926\ V} AuCl_2^- \xrightarrow{1.154\ V} Au$$

The reduction potential of gold is sufficiently high compared to the entire range of reduction potential of the tea polyphenolic flavonoids. So this makes the gold precursor $HAuCl_4^-$ solution easily reducible by the phytochemicals present in tea extract.

### 3.6 Conclusions

Monodispersed gold nanoparticles were synthesized using tea extract of commercially available tea leaves in an aqueous media in a one-pot synthesis and stabilization method at a constant temperature of 25±5˚C without the presence of any external surfactant or reducing agent. The reaction steps are completed within 30 minutes and the particles when analyzed by microscopic studies showed uniform spherical sized particles with an average dimension of ~30 nm. The FT-IR analysis shows that the tea extract is responsible for the reduction of the precursors and the subsequent synthesis of gold nanoparticles. A probable mechanism where the polyol groups of the tea phytochemicals helps in the reduction and stabilization of the gold nanoparticles were explored and it was found that the roles of tea phytochemicals are crucial for the reduction of the gold precursor solution and for stabilization of the same nanoparticles. Modern medicinal uses of metal nanoparticles such as gold are well renowned phenomena, but the toxicity of the chemically synthesized gold nanoparticles prohibits the use of gold nanoparticles for medicinal purposes. Tea is a beverage known for many health benefits and is taken by many people daily in all the continents, the reduction of gold precursor by tea extract can be assumed to produce cytocompatible gold nanoparticles.

# Chapter 4

# Synthesis of Iron oxide Nanoparticles Using Tea Extract

## 4.1 Introduction

Magnetic nanoparticles are an important family of nanomaterials. Magnetic materials with defined nanostructures have been intensively explored due to their multidisciplinary applications. Magnetic nanoparticles are used in magnetic fluids, catalysis, data storage, bio-separation and environmental treatment. Iron is one of the most abundantly available materials on the face of the earth and it is also the most useful and practical magnetic material. Early studies of iron as a nanomaterial consisted of studying the difference in properties from bulk phase to the micro or nano phase. Theories conceived to determine the magnetic property of iron nanoparticles in nano scale were difficult to assess without the proper measurement of size and morphology. But with time the theories governing the magnetization and other properties of iron nanoparticles were fully molded and ever since the research concentration in iron nanoparticles for numerous applications has shown no sign of deceleration

Iron oxide ($Fe_xO_y$) nanomaterials often exhibit high magnetic response when exposed to an external magnetic field and can be used for selective capture of targeting substrates, recyclable nanocatalysis and magnetic photonic purposes (Yi et. al., 2006, Lee et. al., 2008, Ge et. al., 2009, Ge et. al., 2011). When the particle size of $Fe_xO_y$ is below a critical value (~10–20 nm), the magnetic nanoparticles show super paramagnetic behavior when the temperature is above the blocking temperature. No remanence and coercivity would be found in these materials and the aggregation phenomenon of these hybrid particles is negligible at room temperature (Jeong et. al., 2007). In addition, $Fe_xO_y$ nanoparticles are prevalent in molecular imaging as the contrast agents with negative contrast for magnetic resonance imaging (MRI). Furthermore, iron oxide nanoparticles are applied in several biomedical applications like cell labeling, purification and separation of cell populations, targeted drug delivery, hyperthermia etc. For biomedical applications of iron oxide nanoparticles they must possess collective properties of high magnetic saturation, biocompatibility and interactive functions at the surface. Iron oxide nanoparticles have been long synthesized by several physical and chemical methods. The physical methods such gas phase deposition and electron beam lithography are not considered as an effective process as they require elaborate procedure and lack the ability to control the particle size formation. The main chemical method for iron oxide nanoparticle synthesis is the hydrothermal co-precipitation method by which $Fe_xO_y$ nanoparticles can be fabricated by co-precipitation of

$Fe^{2+}$ and $Fe^{3+}$ aqueous salt solutions in alkaline media. This procedure is generally applied for production of iron oxide nanoparticles. Other known chemical process for synthesis of iron oxide nanoparticles involves the use of the reverse micellization process. But the bio-applicability of the iron oxide nanoparticles synthesized by chemical routes are often very low and so the surface of those nanoparticles needs to be modified by using either surfactants or materials which are biologically inert in nature. These surface modification and stabilization process often require complex steps and incur a significantly larger cost and sometime the presence of the still lingering harmful chemicals can make the nanoparticles unsuitable for biomedical theranostic and diagnostic applications. This has encouraged researchers to look for more environmentally beneficial synthesis procedure. This search for greener synthesis routes led to the exploration of synthesis of iron nanoparticles by Sorgum bean extract [Njagi et al., 2011], Alfalafa plant extract [Ascencio et al., 2007], commercially available polyphenols like Grape seed proanthocyanidin [Menon et al., 2012] and epicatechin [Varma et al., 2010] and glucose [Shen et al., 2010] and nickel nanoparticles by Burberry tannin [Liao et al., 2012]. Tea has a diverse constituent of water soluble and biodegradable polyphenolic flavonoids which are water soluble at room temperature unlike other polymers. These polyphenolic flavonoids can form complex with iron oxide nanoparticles (Ahmmad et al., 2013) and thereafter can help in stabilization of the particles. Tea with its myriad ranges of polyphenolic flavonoids, have a diverse range of reduction potential, thus can be used as a reducing agent in an aqueous media for producing iron oxide nanoparticles. In this study, commercially available tea leaf extract used to synthesize iron oxide nanoparticles in an aqueous system without the presence of any surfactant or dispersing medium. The main objective of this chapter is to study the synthesis of iron oxide nanoparticles in a aqueous medium using tea extract and to characterize the as synthesized iron oxide nanoparticles to confirm the formation of the iron oxide nanoparticles.

## 4.2 Experimental Section

### 4.2.1 Materials

The required chemicals were purchased from the following sources: Ferric nitrate ($Fe(NO_3)_3$), Ferrous sulfate, hepta hydrate ($FeSO_4.\ 7\ H_2O$) and sodium hydroxide( NaOH) was purchased from Merck Ltd. Each with 99% assay. Commercially available tea leaf (Red Label) from Tata India Ltd., with 99% purity was purchased. Ultrapure water of 18.2 MΩ cm resistivity and 6.4-6.5 pH was used for all the experiments. The constant temperature of 25±0.5˚C was maintained throughout the experiments. The iron precursor was used as received but the tea leaf extract was prepared in ultrapure water explained in detail in the next section.

### 4.2.2 Synthesis Techniques

#### 4.2.2.1 Preparation of Tea leaf extract

Tea leaves from commercially available brand Red Label (Tata India Ltd., 99% purity) was purchased and 2 grams of tea leaf was mixed in 100 ml of ultrapure water (2% w/v), and then heated at 100˚C for 20 min in a hot water bath. The residue was separated by filtration first through Whatman No. 42 filter paper and secondly through a filter of 0.45 μm pore size. Finally the leaf extract was centrifuged at 20,000 rpm (Sigma, Model No. 3-30K, Germany) for 15 minutes to remove any ultrafine suspended particles. The pH of the tea extract was determined at almost neutral ~6.5.

#### 4.2.2.1 Synthesis of Iron Oxide ($Fe_xO_y$) Nanoparticles

Iron oxide nanoparticles were prepared from aqueous $Fe(NO_3)_3$ solution with a constant concentration of 0.1mM as a precursor and using the as prepared tea extract in the previous section as a reducing agent in aqueous medium. A constant ambient temperature of 25˚C was maintained throughout the process, where the $Fe(NO_3)_3$ solution was stirred continuously and 10 μl of tea extract was added to the solution. The synthesis of iron oxide nanoparticles does not require any lag period such as in the case of gold nanoparticles, the color change is instantaneous from yellow to dark brown tending towards black. The precursor concentration does not have much effect on the change in physical appearance but with the increase in addition of tea extract from 10 to 20, 30, 40 and 50 μl the color of the solution deepens. The resulting solution was sonicated by using a probe type sonicator using 260 watt for 10 min. After a waiting period of 30 minutes the solution containing the particle were centrifuged at 25,000 rpm for 15 minutes, and washed with double distilled water thrice. This as synthesized iron oxide nanoparticles does not respond to the presence of external magnetic field. A control experiment was performed using $Fe(NO_3)_3$ and $FeSO_4$ solution at 2:1 ratio in a hydrothermal co-precipitation approach. The solutions were heated at 60˚C in a bath sonicator as direct application of magnetic stirring would inhibit the separation process, and slowly NaOH (2M) solution was added to the aqueous solution for the co-precipitation process. The change in color by precipitation of black particles indicated the formation of iron oxide nanoparticles. The resulting solution was sonicated by using a probe type sonicator using 260 watt for 10 min. Then the particles can be clearly separated by using an external magnetic field. After a waiting period of 30 minutes the solution containing the particle were centrifuged at 25,000 rpm for 15 minutes, and washed with double distilled water thrice.

### 4.2.3 Particle Characterization

Particle size measurement was carried out by dynamic light scattering (DLS) using Malvern Zeta Size Analyzer, U.K. (Nano ZS). The particles were characterized by UV-vis NIR Spectroscopy (Shimzadu-3600), FTIR Spectroscopy (Thermo-Fischer-Nicolet iS10) ), X-ray Diffraction (XRD) (Philips, Pw, 1830 HT) and Energy-dispersive X-ray diffraction spectroscopy (EDX) attached with the field emission scanning electron microscope (FESEM) (Nova Nano SEM/ FEI) used to observe the size and shape of the particles.

## 4.3 Results and Discussion

### 4.3.1 Characterization of Nanoparticles by UV-vis Spectroscopy

UV-vis spectroscopy was used for analysis of the iron oxide nanoparticles formed using the tea extract upon $Fe(NO_3)_3$ 0.1 mM solution. Absorption measurement of the control $Fe(NO_3)_3$ blank solution has an absorption spectra beginning at 500 nm and increasing by 300 nm wavelength. The absorption spectra of the iron oxide nanoparticles are shown in Figure 4.1. The control solution of iron oxide nanoparticles synthesized using chemical route also shows similar absorption spectra. All the absorption spectra show a broad absorption at a higher wavelength and there was a soft rise at around ~300 nm but no sharp absorption peak is found in lower wavelengths. The lower part of the photograph shows the change in the physical appearance of the iron precursor solution with the addition of the tea extract. As the change in physical appearance is instantaneous there is no indication of any lag phase as seen during the synthesis of gold nanoparticles. The UV-vis spectrum of the tea extract or leaf broth shows that there is a $\lambda_{max}$ at around 270 nm which may be due to the presence of the phytochemicals in the tea extract.

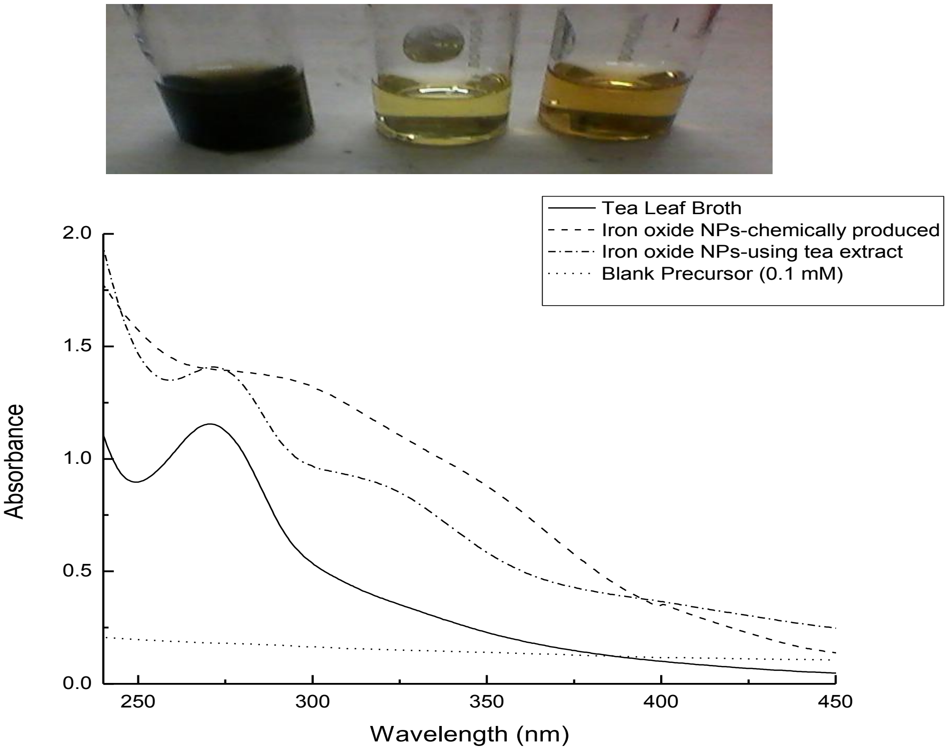

**Figure 4.1:** UV-vis absorption spectra of $Fe(NO_3)_3$ blank control solution, control tea extract, $Fe_xO_y$ NPs synthesized using tea extract and $Fe_xO_y$ NPs synthesized using chemical methods respectively in a upward direction. Inset picture shows $Fe_xO_y$ NPs, $Fe(NO_3)_3$ blank, tea extract from right to left.

### 4.3.2 Characterization of Particles by XRD

As synthesized iron oxide nanoparticles using tea extract were characterized by X-ray diffraction (XRD) as shown in Figure 4.2. Scans were performed over a 2-theta ranging from 20 to 70˚. The XRD pattern of the as synthesized iron oxide nanoparticles shows that it is a mixture of magnetite ($Fe_3O_4$) and hematite ($Fe_2O_3$). The different phase of hematite in the mixture corresponds to different phase structure such as: hexagonal $Fe_2O_3$ (JCPDS PDF No. 76-1821 & 40-1139), rhombohedral $Fe_2O_3$ (JCPDS PDF No. 84-0308) and monoclinic $Fe_2O_3$ (JCPDS PDF

No. 16-0653). The magnetite on the other hand shows only cubic structure (JCPDS PDF No. 40-1139 & 79-0417). The pattern depicts several of the major peaks at the 2θ degree 33.16°, 33.33°, 34.37°, 35.45°, 35.19°, 38°, 40.32°, 41.19°, 42.94°, 45.8°, 48.4°, 57.16°, 57.61°, 62.72°, which respectively corresponds to the (112), (104), (106), (113), (110), (040), (115), (200), (116), (024), (118), (511), (300), (003), (440) planes for the hematite ($Fe_2O_3$) group. The pattern also shows the peaks at 30.087°, 35.31°, 35.54°, 57.17°, 62.73° 2θ degree which corresponds to the (220), (311), (511), (440) plane for the magnetite ($Fe_3O_4$) portion of the mixture.

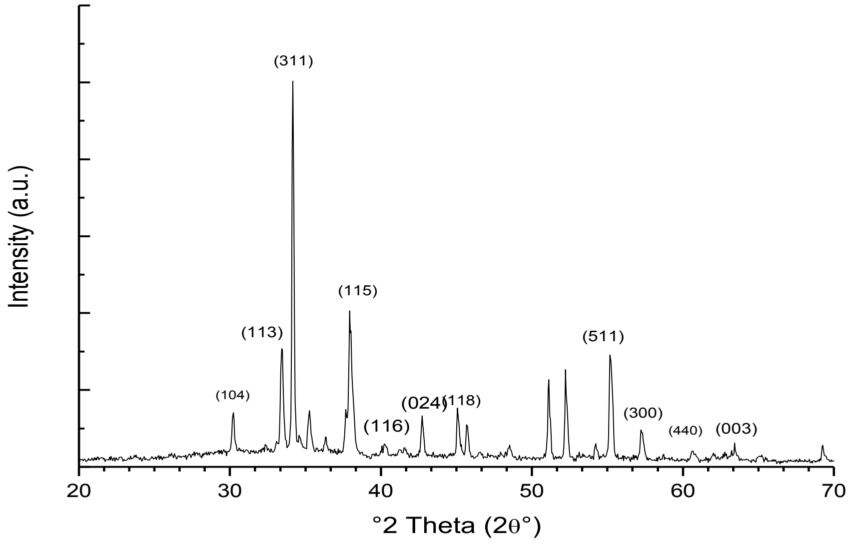

**Figure 4.2:** XRD pattern of iron oxide nanoparticles synthesized using tea extract.

### 4.3.3 Characterization of Particle Size and Morphology

The physical properties like size and morphology of the iron oxide ($Fe_xO_y$) were analyzed by field emission scanning electron microscopy (FESEM) and dynamic light scattering (DLS) techniques. The FESEM measurement of the iron oxide nanoparticles synthesized by reducing $Fe(NO_3)_3$ 0.1 mM solution are spherical in shape within the size range of 30-70 nm with an average size at about ~50 nm. The FESEM image (Figure 4.3(a)) shows that the as synthesized iron oxide nanoparticles are in accordance with the data determined by the dynamic light scattering (DLS) analysis method of size measurements. The DLS data is shown in Figure 4.3(c). The formation of iron oxide nanoparticles with polyphenolic flavonoids from tea extract proceeds with complexation of the iron precursor with the functional groups and then subsequent reduction and further capping of the nanoparticles with polyphenolic flavonoids from tea extract. This capping and complexation of the iron oxide nanoparticles with the tea phytochemicals might be responsible for the increased size of the nanoparticles rather than the actual size of the iron oxide nanoparticles and the agglomeration seen in the image might be also the result of the capping effect. The as synthesized nanoparticle suspension after centrifugation and further sonication by a probe sonicator was analyzed again by FESEM and the image Figure 4.3 (b) shows the microscopic image. The FESEM image shows that the iron oxide particle after sonication at 260W by a probe sonicator for 20 minutes becomes fairly well dispersed but the dimension of the particle remains in the similar range of 30-60 nm. Additionally the EDX analysis of the data attached with the FESEM analysis of the iron oxide nanoparticles shown in the Figure 4.3 (d) confirms about the iron oxide nanoparticles.

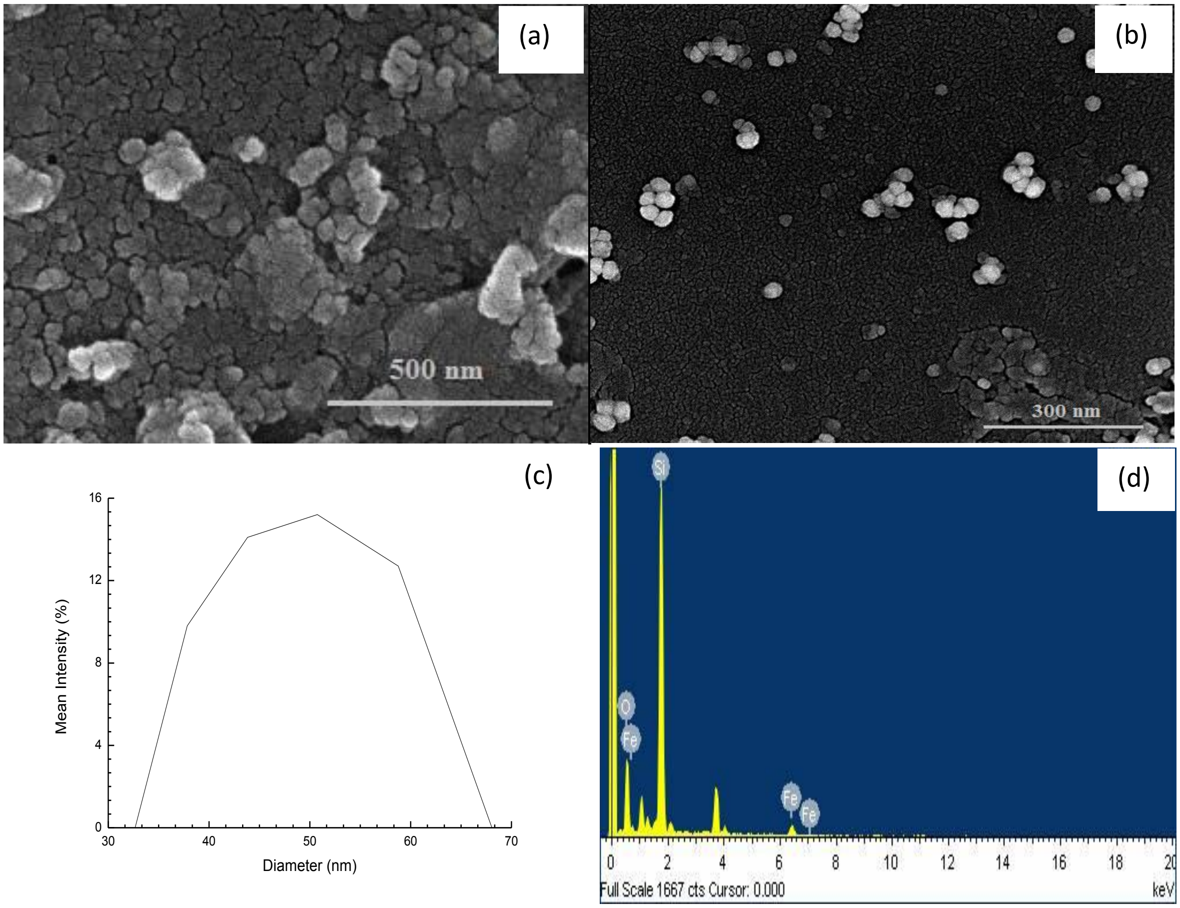

**Figure 4.3:** FESEM images of (a) as synthesized iron oxide nanoparticles, (b) sonicated iron oxide nanoparticles, (c) DLS data of the iron oxide nanoparticles, (d) EDX analysis of iron oxide nanoparticles.

### 4.4 Characterization of Particles by FT-IR Spectroscopy

FT-IR characterization was done to get an idea about the functional groups present in the tea extract and the role of those groups in formation of the iron oxide nanoparticles. The FT-IR spectra of the fresh tea extract before and after reduction of $Fe(NO_{3)3}$ solution are shown in Figure 4.5. The absorption bands in Figure 4.5(a) are observed in the region of 1000-1800 cm$^{-1}$ are 1683, 1623, 1362, 1213 and 1150 cm$^{-1}$. The absorption bands corresponds to different group frequency region, such as the absorption bands at 1683, 1623, 1362, 1213 cm$^{-1}$ are associated with the stretching vibrations of the –C=C–C=O and –C=C– in ring aromatic groups, –C–C– in ring aromatic group, C–O stretch of esters and ethers groups and C–O stretch of polyols groups respectively. In particular the 1213 cm$^{-1}$ band arises most probably from the C–O group of polyols such as hydroxyflavones and catechins, which are the main groups of functional material in tea extract. After the reduction of the iron precursor solution the predominant peaks disappear in the Figure 4.4(b). This may be due to the involvement of the functional groups in the bioreduction of the iron oxide nanoparticles. A probable mechanism of reduction is explained later in the chapter.

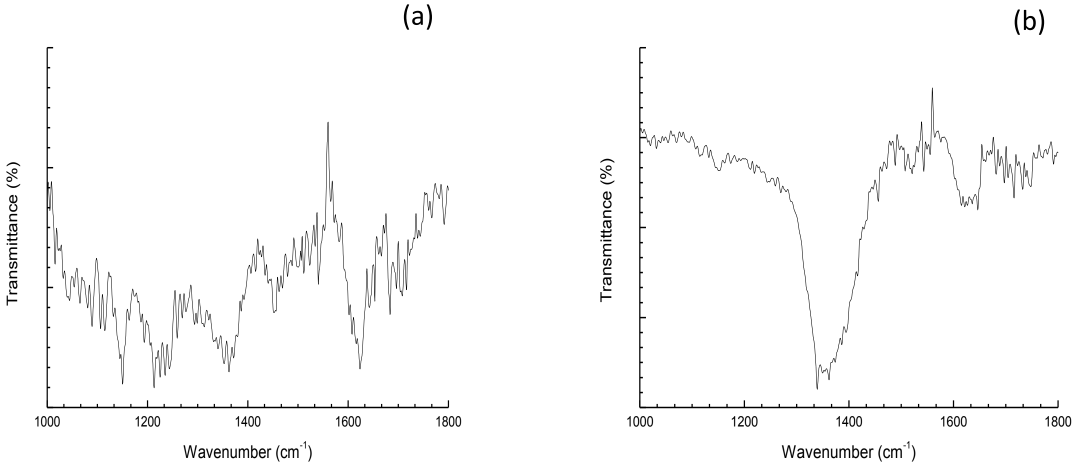

**Figure 4.4:** FT-IR images of (a) Tea extract, (b) Iron oxide nanoparticles synthesized using tea extract.

### 4.5 Possible Mechanism of Nanoparticle Synthesis

The phytochemicals present in tea extract plays a major role in synthesis and capping of the iron oxide nanoparticles. As previously stated the polyphenolic flavonoids in tea extract has reduction potential ranging from 0.3 to 0.8 V. The reduction potential of iron salt precursor solution is -0.44 V, sufficient to be reduced by tea phytochemicals. A plausible formation mechanism of iron oxide nanoparticles by tea extract is presented in the following Figure 4.4 supposing that the epigallocatechin gallate (EGCG), gallocatechin gallate (GCG), catechin and other theaflavins work as both reducing and capping agent.

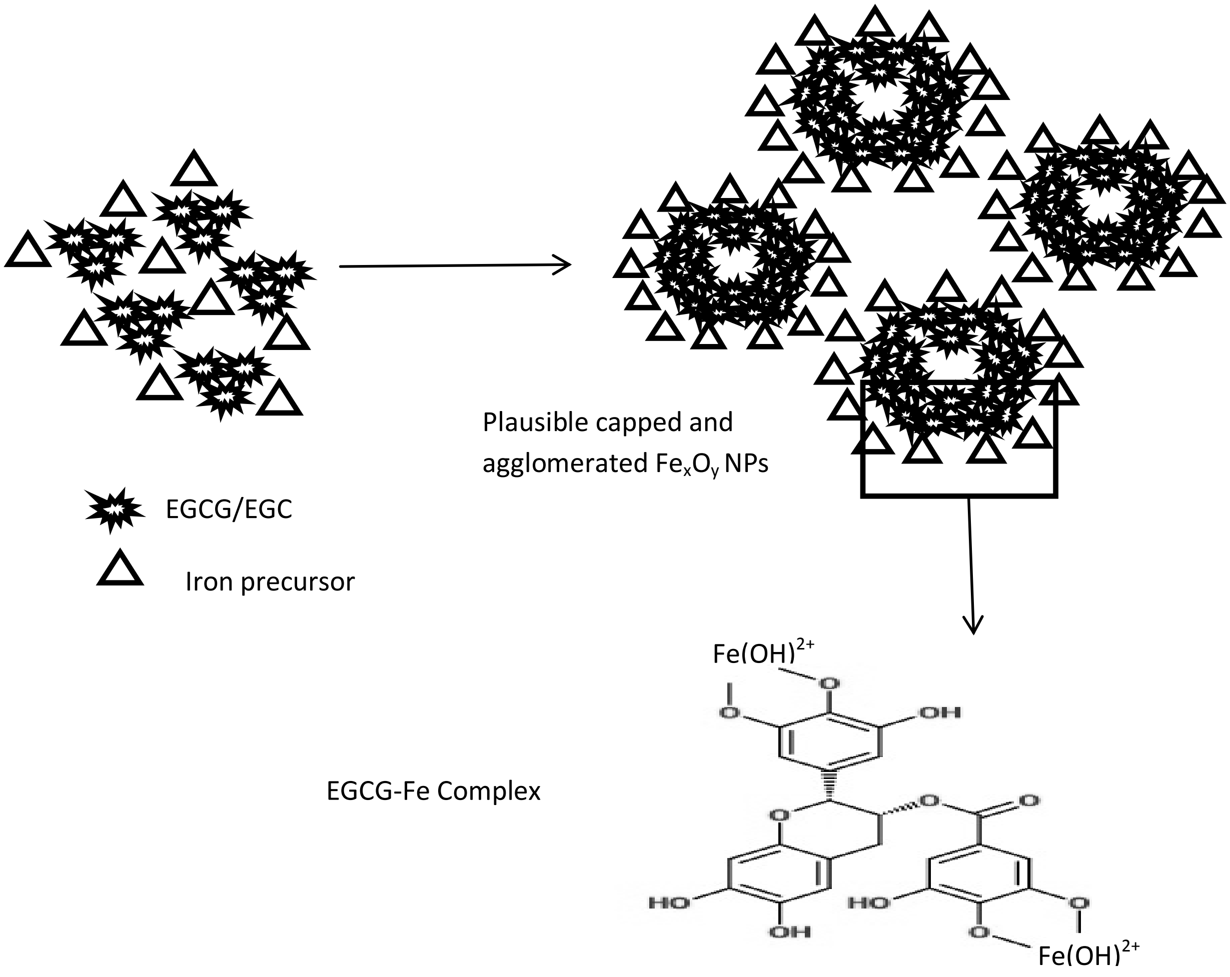

**Figure 4.5:** Plausible schematic of iron oxide nanoparticle formation mechanism by reducing iron precursor solution by tea extract.

The initial octa-hedral aqua complex of iron (III), $Fe(H_2O)_6$, which is formed in water instantaneously decomposes into several soluble low-molecular- weight species (such as $[Fe(OH_2)(OH)]^{2+}$, $[Fe(OH_2)_4(OH)_2]^{+}$)via deprotonation of coordinated water molecule. The hydrolyzed iron species could form a complex with B and D ring of deprotonated catechins and theaflavins or polyol groups of the tea extract at halfway of the process. As the other side of catechin group (A-ring side) is comparatively hydrophobic in nature, a tendency of aggregation might occur forming a structure shown in Figure 4.4. The initially formed iron species $[Fe(OH)_2]^{+}$ might go through a phase transformation forming primary particles ($Fe_2O_3$, $Fe_3O_4$) of several nanometer dimension. These primary particles have high surface energy and aggregate quickly to minimize their surface energy which may be the reason behind the aggregation of the nanoparticles and subsequent increase in dimension. As we have already discussed in case of gold nanoparticles that EGCG and epigallocatechin (EGC) provides the most stabilization effect we might assume that the same occurs in case of iron oxide nanoparticles.

## 4.6 Conclusions

Iron oxide nanoparticles containing a mixture of both hematite ($Fe_2O_3$) and magnetite ($Fe_3O_4$) group of nanoparticles were synthesized in a one-step green route synthesis of magnetic nanoparticle by using commercially available tea extract at a constant temperature of 25±5˚C without the presence of any external surfactant or reducing agent.. The tea extract not only reduces the iron precursor $Fe(NO_3)_3$ 0.1 mM solution by complexation with the initially formed iron species, but later acts as a capping agent for the newly formed iron oxide nanoparticles. The FT-IR analysis shows that the tea extract is responsible for the reduction of the precursors and the subsequent synthesis of iron oxide nanoparticles. The resulting capped and agglomerated iron oxide nanoparticles showed random shaped particles with average dimension at about ~50 nm. The capping of the iron oxide nanoparticles by tea extract covers the easily reactive surface of the particles protecting it from further oxidation. This biogenesis of iron oxide nanoparticles provides a biocompatible pathway of iron oxide nanoparticle formation which is currently the major attention holder in the field of nano medicine.

# Chapter 5

# Synthesis of Gold-Iron oxide Composite Nanoparticles Using Tea extract

## 5.1 Introduction

Heterogeneous nanoparticles with two or more particles in close contact are currently at the center of attention in nanotechnology owing to their unique electronic, magnetic, optical and catalytic properties present in the structure. To design the advanced composite nanomaterials it is important to choose two such materials whose interparticle close interaction would be beneficial for the application of the nanoparticle. Noble metal-magnetic nanocomposites with defined nanostructures have been intensively investigated due to their multi-disciplinary applications, such as magnetic fluids, catalysis, data storage, bioseparation, and environmental treatment. The magnetic iron oxide nanoparticles are favorable among the magnetic nanoparticles for constructing magnetic hybrid nanocomposites due to their intrinsic magnetic properties related with size and surface molecules. These magnetic nanocomposites also show superparamagnetism when the dimension of the iron oxide nanoparticles is below a critical value ~10-20nm. Iron oxide nanoparticles are prevalent in molecular imaging as a contrast agent with negative contrast for magnetic resonance imaging. The greatest weakness of iron is its reactivity specifically with respect to water and oxygen. This general weakness is amplified to multifold in case of iron oxide nanoparticles where the high reactivity can be advantageous for a catalysis process, but the iron oxide nanoparticles can rapidly and completely oxidize in water or oxygen. This reactivity of iron oxide nanoparticles can make the particles cytotoxic in nature and hinders with the biomedical application of the nanoparticles.

Gold is a noble metal, and remains inert in physiological condition, facilitating the application of gold nanoparticles in cellular optical imaging, hyperthermia, and sensitive bio-detection for DNA, proteins or other biomolecules. The plasmonic resonance peak of Au could be shifted to the NIR region by tuning the proximities and geometries of the Au nanoparticles. It is reported that presence of gold (Au) as a shell layer or composite material could also provide a strong plasmonic resonant optical response to the nanoparticle, wherein the resonant frequency could be determined by the geometry and dielectric properties of the core, as well as the surrounding medium. Therefore, the thriving combination of Au and $Fe_xO_y$ are promising to obtain Au–$Fe_xO_y$ hybrid nanocomposites with expedient and opportunous properties from both individual Au and $Fe_xO_y$ nanoparticles. In this chapter the synthesis method for a one step synthesis of gold-iron oxide composite nanoparticle using tea extract is discussed. In the previous chapter the synthesis of single gold and iron oxide nanoparticle synthesis using tea extract has been discussed. Here the same steps have been followed using tea extract from commercially available tea leaf to produce gold-iron oxide (Au-$Fe_xO_y$) composite nanoparticle in an aqueous system without the presence of any external surfactant or reducing agent.

## 5.2 Experimental Section

### 5.2.1 Materials

The required chemicals were purchased from the following sources: Ferric nitrate ( $Fe(NO_3)_3$), Ferrous sulfate, hepta hydrate ($FeSO_4 . 7 H_2O$) and sodium hydroxide( NaOH) was purchased from Merck Ltd. Each with 99% assay along with chloroauric acid ($HAuCl_4$, $xH_2O$) from Sigma-Aldrich with 99% assay. Commercially available tea leaf (Red Label) from Tata India Ltd., with 99% purity was purchased for preparing the tea extract. Ultrapure water of 18.2MΩ cm resistivity and 6.4-6.5 pH was used for all the experiments. The constant temperature of 25±0.5˚C was maintained throughout the experiments. The iron and gold precursor was used as received but the tea leaf extract was prepared in ultrapure water explained in detail in the next section.

### 5.2.2 Synthesis Techniques

#### 5.2.2.1 Preparation of Tea leaf extract

Tea extract from commercially available tea leaves were prepared by the method described in Chapter 1, Section 3.2.2.1.

#### 5.2.2.1 Synthesis of Nanoparticles

Gold-iron oxide composite nanoparticles were prepared from aqueous $Fe(NO_3)_3$ solution with a constant concentration of 0.1mM and $HAuCl_4$ with a constant concentration of 0.001mM as the precursors and using the as prepared tea extract in the previous section as a reducing agent in aqueous medium. A constant ambient temperature of 25˚C was maintained throughout the process, where the $Fe(NO_3)_3$ and $HAuCl_4$ solution in different ratios (2:1, 1:1, 1:2, 1:4 v/v) was stirred continuously and 10 µl of tea extract was added to the solution. The synthesis of gold-iron oxide composite nanoparticles shows no such lag period as in the case of gold nanoparticles, the color change is instantaneous from yellow to shades of brown and finally brown with a hint of red or pink due to the presence of gold nanoparticles for the precursors in 4:1 (v/v) ratio. The tea extract concentration does not have much effect on the change in physical appearance but with the precursor ratio increases maintaining the same concentration color of the solution deepens. The resulting solutions were sonicated by using a probe type sonicator using 260 watt for 10 min. After a waiting period of 30 minutes the solutions containing the particle were centrifuged at 25,000 rpm for 15 minutes, and washed with double distilled water thrice. This as synthesized gold-iron oxide composite nanoparticles does not respond to the presence of external magnetic field. As seen from the synthesis of gold and iron oxide nanoparticles here also tea polyphenolic flavonoids are responsible for the probable capping and agglomeration mechanism, resulting in the amorphous nature of the solution and might be responsible for the enhancement in particle size. To remove the tea phytochemicals from the final washed particles were heat treated at 450˚C for 30 min in air, the resulting composite nanoparticles response to external magnetic field, are well dispersed when sonicated using a 260 watt probe sonicator for 5 min and can be separated by an external magnetic field. The resulting particle was studied for morphological information.

### 5.2.3 Particle Characterization

Particle size measurement was carried out by dynamic light scattering (DLS) using Malvern Zeta Size Analyzer, U.K. (Nano ZS). The particles were characterized by UV-vis NIR Spectroscopy (Shimzadu-3600), FTIR Spectroscopy (Thermo-Fischer-Nicolet iS10) ), X-ray Diffraction analysis(XRD) (Philips, Pw, 1830 HT) and Energy-dispersive X-ray diffraction spectroscopy (EDX) attached with the field emission scanning electron microscope (FESEM) (Nova Nano SEM/ FEI) used to observe the size and shape of the particles.

## 5.3 Results and Discussion

### 5.3.1 Characterization of Au-$Fe_xO_y$ Composite Nanoparticles by UV-vis Spectroscopy

UV-vis spectroscopy was used for the characterization of the gold-iron oxide (Au-$Fe_xO_y$) composite nanoparticles formed using tea extract upon different ratio of iron and gold precursor solution. Absorption measurements of the Au-$Fe_xO_y$ composite nanoparticles shows different absorption bands for the different ratio of iron and gold precursor ratio used in the solution. The absorption spectra of these particles are shown in Figure 5.2. For the $Fe(NO_3)_3$ : $HAuCl_4$ ratio 2:1and 1:1 the physical appearance is dark brown, and the absorption spectra shows a broad absorption band starting at 500 nm with a small peak at around 300 nm for the iron oxide nanoparticles and another peak at around 540 nm confirming the presence of gold nanoparticles. For the $Fe(NO_3)_3$ : $HAuCl_4$ ratio 1:2 the color of the solution changes to greenish brown and the absorption spectra shows a sharp absorption band with the $\lambda_{max}$ of the composite particles at around 560 nm. Thus the absorption peak shifts towards longer wavelength (red shift) when the gold precursor ratio increases in the solution.

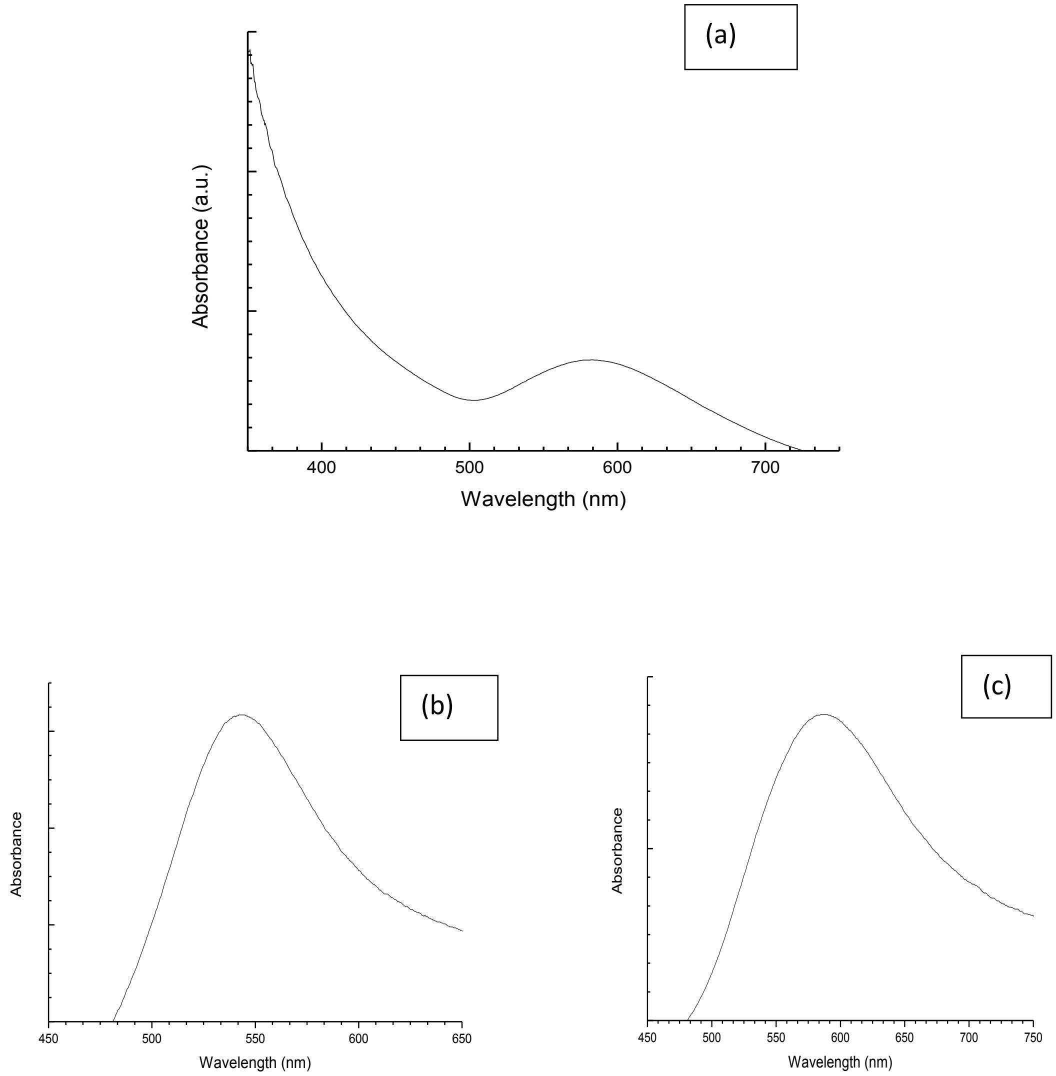

**Figure 5.1:** UV-vis spectroscopy analysis of gold-iron oxide (Au-$Fe_xO_y$) nanoparticles as synthesized by tea extract reducing different solution with $Fe(NO_3)_3$ : $HAuCl_4$ ratio 2:1 and 1:1(a), 1:2 (b), 1:4 (c) respectively.

This spectra also shows no sign of the iron oxide absorption spectra, thus it can be assumed that the gold nanoparticles has complexed with the iron oxide nanoparticles capped by tea polyphenolic flavonoids suppressing or covering the surface of the iron oxide nanoparticles. For the solution with $Fe(NO_3)_3$ : $HAuCl_4$ ratio 1:4 the physical appearance is brownish pink with clearly visible presence of gold nanoparticles due to the red or pink coloration blurred by the presence of iron oxide nanoparticle present. This spectrum shows an absorption peak at around 570 nm but no significant absorption spectra for iron oxide nanoparticles appeared in the visible region. Thus a capping or complexation mechanism of the iron oxide nanoparticles either by tea phytochemicals or by gold nanoparticles can be assumed to have happened here masking the absorption spectra of the iron oxide nanoparticles. The sharpness of the peak was reduced in case of absorption spectrum of gold. The presence of iron oxide might be affecting the increase in $\lambda_{max}$ of the absorption spectra and the presence of a higher concentration of iron oxide may have resulted in the formation of bigger Au-$Fe_xO_y$ composite nanoparticles.

### 5.3.2 Characterization of Au-$Fe_xO_y$ Composite Nanoparticles by XRD

Au-$Fe_xO_y$ Composite Nanoparticles synthesized in a one-step green route process by tea extract were characterized by X-ray diffraction analysis (XRD) and the Figure 5.3 shows the XRD pattern of those particles. The scans were performed were performed over a range of 2-theta 10 to 80˚. The pattern shows the presence of gold (Au) nanoparticles (02-1095 from JCPDS PDF number) and iron oxide ($\alpha$-$Fe_2O_3$ and $\gamma$-$Fe_2O_3$) nanoparticles (JCPDS PDF No. 13-534, 25-1402, and 8-98). Both $\alpha$-$Fe_2O_3$ and $\gamma$-$Fe_2O_3$ phases of iron oxide nanoparticles exist in the suspension. The pattern shows several major peaks among them the $2\theta$ degrees of 38.23˚, 44.35˚, 64.66˚ and 77.55˚ corresponds to the (111), (200), (220) and (311) planes for the gold nanoparticle. Whereas the $2\theta$ degree of 20˚, 33 ˚ belongs to (113) and (220) of $\gamma$-$Fe_2O_3$ phase of nanoparticles and 25.9˚, 46.79˚, 53.81˚, 77.68˚ matches the (102), (118), (116) and (220) of $\alpha$-$Fe_2O_3$ phase of nanoparticles. The dominant crystal planes are (220) & (111) and the particles have face centered cubic (fcc) structure.

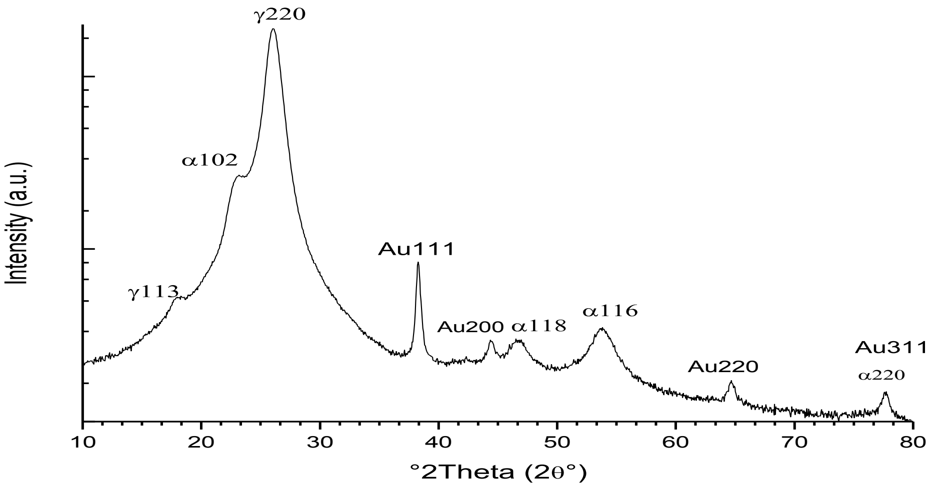

**Figure 5.2:** XRD pattern of Au-$Fe_xO_y$ Composite Nanoparticles synthesized using tea extract

### 5.3.3 Characterization of Particle Size and Morphology

The composite gold-iron oxide nanoparticles were analyzed by field emission scanning electron microscopy (FESEM) and dynamic light scattering (DLS) techniques. The FESEM measurement of Au-$Fe_xO_y$ composite nanoparticles by reducing the 1:2 ($Fe(NO_3)_3$:$HAuCl_4$) ratio precursor solution by tea extract is depicted in Figure 5.4(a). The FESEM data shows that the as synthesized nanocomposite particles are highly agglomerated and polydispersed in aqueous medium. The particles have a size range of about 10 to 40 nm and some particles are seen below the range of 10 nm.

This data from the FESEM image collaborates with the data analyzed by dynamic light scattering (DLS) technique (Figure 5.4(c)). The particles are seen spherical in shape and polydispersed. The polyphenolic flavonoids from tea extract encapsulates the composite nanoparticle by complexation with possibly the iron precursor as stated in previous chapter, and probably the gold nanoparticles were encapsulated by the tea phytochemicals and subsequently the gold and iron nanoparticles forms the composite nanoparticle in a close interacting framework of tea polyphenolic flavonoids. The heat treated Au-$Fe_xO_y$ composite nanoparticles when analyzed by FESEM technique shows that (Figure 5.5) during heat treatment the size of the nanoparticle increases to an average of 120-130 nm, however the nanoparticles becomes monodispersed. The EDX analysis of the data attached with the FESEM analysis of the composite nanoparticles confirms about the Au-$Fe_xO_y$ composite nanoparticle and ratio of the gold-iron oxide ratio is found to be 4:2 or 2:1 which confirms with the experimental data. The EDX data is shown in Figure 5.4(d).

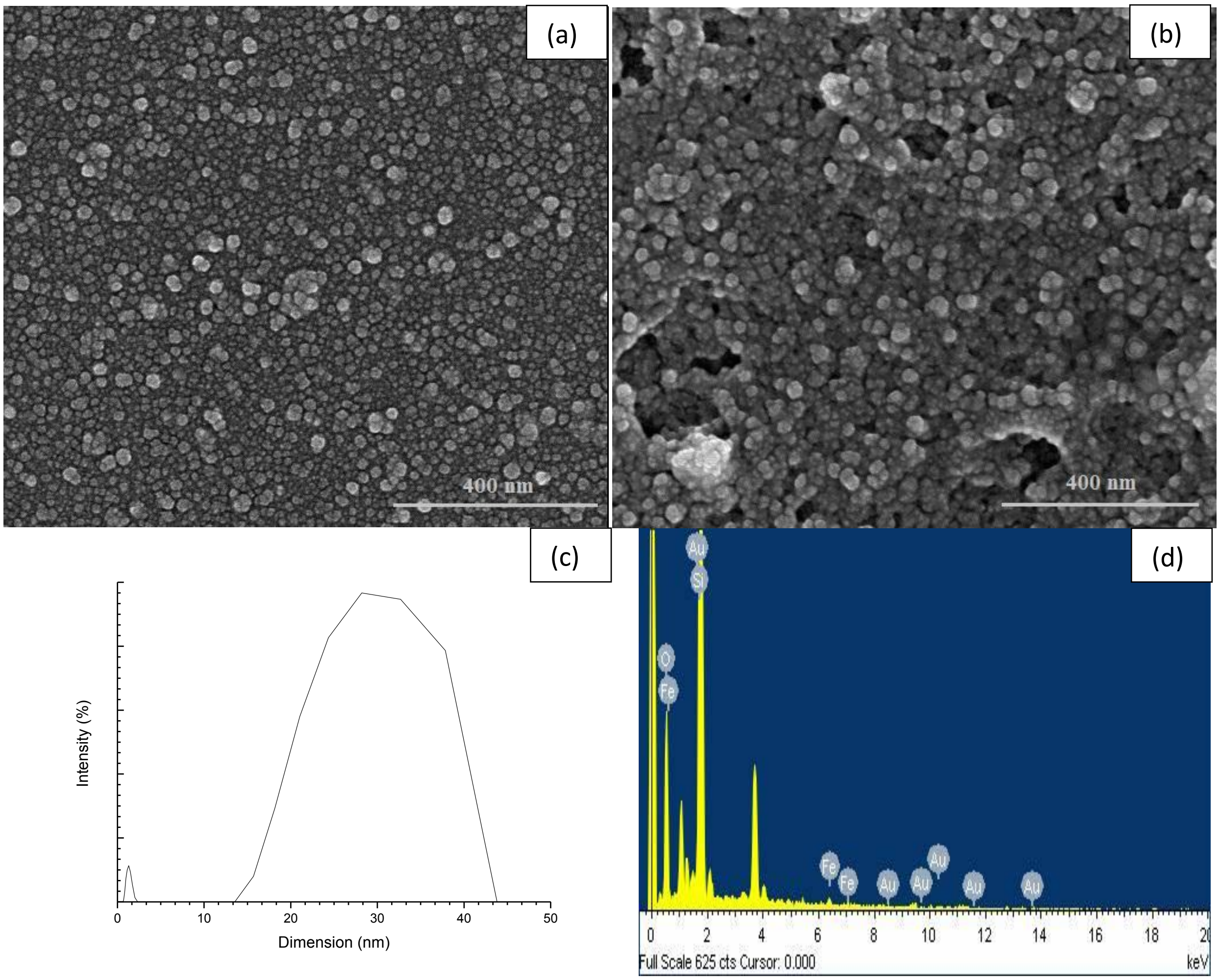

**Figure 5.3:** FESEM images (a, b), DLS data (c), EDX data (d) of Au-$Fe_xO_y$ composite nanoparticles synthesized using tea extract.

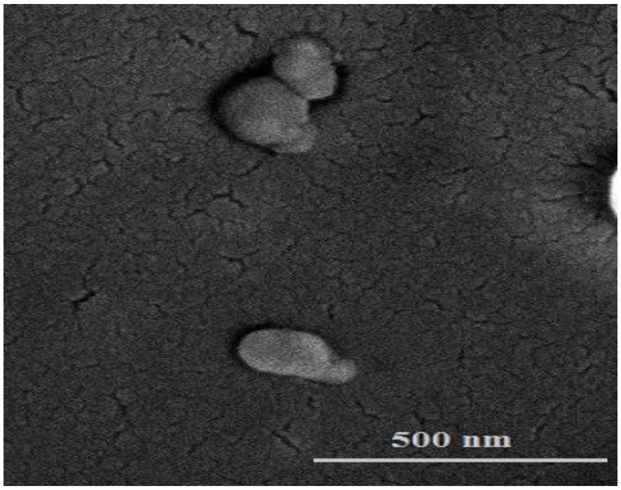

**Figure 5.4:** FESEM image of heat treated Au-$Fe_xO_y$ composite nanoparticles.

## 5.5 Characterization of Particles by FT-IR Spectroscopy

FT-IR characterization was done to get an idea about the functional groups present in the tea extract and the role of those groups in formation of the gold-iron oxide composite nanoparticles. The FT-IR spectra of the fresh tea extract before and after reduction of $HAuCl_4$ and $Fe(NO_{3)3}$ solutions are shown in Figure 5.5. The absorption bands in Figure 5.5(a) are observed in the region of 1000-1800 $cm^{-1}$ are 1683, 1623, 1362, 1213 and 1150 $cm^{-1}$. The absorption bands corresponds to different group frequency region, such as the absorption bands at 1683, 1623, 1362, 1213 $cm^{-1}$ are associated with the stretching vibrations of the –C=C–C=O and –C=C– in ring aromatic groups, –C–C– in ring aromatic group, C–O stretch of esters and ethers groups and C–O stretch of polyols groups respectively. In particular the 1213 $cm^{-1}$ band arises most probably from the C–O group of polyols such as hydroxyflavones and catechins, which are the main groups of functional material in tea extract. After the reduction of the precursor solutions the predominant peaks disappear in the Figure 5.5(b). This may be due to the involvement of the functional groups in the bioreduction of the precursor solutions, whereby they themselves get oxidized to α, β-unsaturated carbonyl groups leading to a broad peak at 1646 $cm^{-1}$. The FT-IR data of Au-$Fe_xO_y$ composite nanoparticles also show presence of some functional material from tea extract. So it can be assumed that those functional groups are involved in plausible capping and complexation of the Au-$Fe_xO_y$ composite nanoparticles.

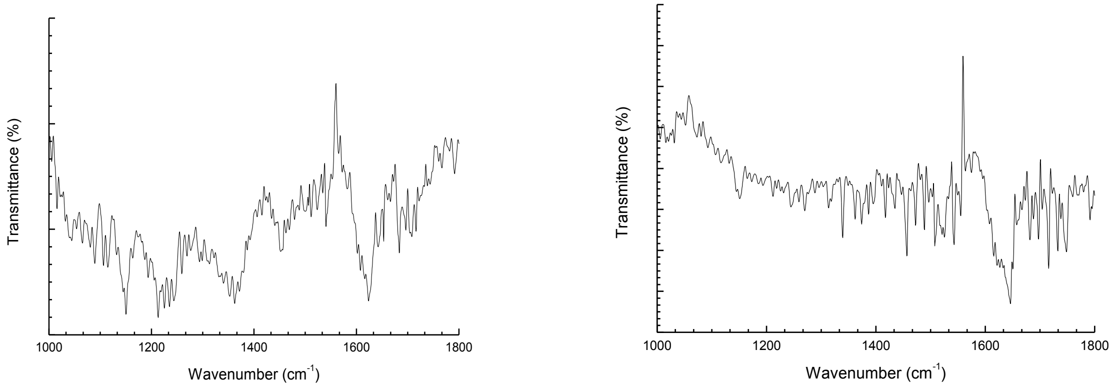

**Figure 5.5:** FT-IR images of (a) Tea extract, (b) Au-Fe$_x$O$_y$ composite nanoparticles synthesized using tea extract.

## 5.6 Conclusions

A novel one-step synthesis of gold-iron oxide (Au-Fe$_x$O$_{y)}$ nanoparticles by a green route method has been used in this study. Tea extract of commercially available tea leaf were used to reduce the gold HAuCl4 and Fe(NO3)3 precursor solution simultaneously in a aqueous media under a constant temperature without any external surfactant or dispersing media to produce Au-Fe$_x$O$_y$ composite nanoparticles. The presence of iron oxide as a composite in close interacting structure tunes the plasmonic properties of the nanoparticle. The absorption peak gets red-shifted to 570 nm depending on the ratio of gold precursor increase. The as synthesized particles are in a agglomerated state and are in polydispersed condition as seen from microscopic analysis due to the complexation and capping mechanism of phytochemicals present in the tea extract. In the as synthesized state the average size of the Au-Fe$_x$O$_y$ composite nanoparticles is between the ranges of 10-40 nm and there are also the presence of some below 10 nm particles as observed from DLS data. The FT-IR analysis shows that the tea extract is responsible for the reduction of the precursors and the subsequent synthesis of gold-iron oxide nanoparticles. However, when the particles are heat treated to remove the tea phytochemicals aggregating the nanoparticles the particle undergoes ripening stages and emerges with increased dimension of about 120-130 nm. The presence of both gold and iron oxide material in the same particle is confirmed by both XRD analysis and EDX analysis. The increase in absorption spectra and total absence of iron oxide spectra might hint at the possibility of a core/shell like formation with non-uniform shell structure by Au nanoparticles over a core of Fe$_x$O$_y$ nanoparticles.

# Chapter 6

# Conclusions and Suggestions for Future Work

## 6.1 Conclusions

The major outcome of this work is the development of a novel green route synthesis method of gold-iron oxide (Au-$Fe_xO_{y)}$ composite nanoparticles in a simple aqueous based synthesis technique using a common household product as a source of both reducing agent, surfactant and capping agent The overall conclusion of the work done in this study is as follows.

In an attempt to find natural, environmentally benign and easily available plant-based agents for metal nanoparticle synthesis, we have demonstrated the superb efficiency of certain commercially available tea leaf extract in the rapid synthesis of stable gold (Au) nanoparticles possessing a spherical morphology. Based on our studies, together with evidence obtained from FTIR, we propose that the main biomolecules responsible for the nanoparticle synthesis were the polyphenolic flavonoids, which are present in comparable concentrations in the tea leaf extract. The particle was found to be fairly monodispersed with the average size distribution of ~30 nm. The concentration of precursor solution also played a major role the in the formation of nanoparticles. With the optimum minimum concentration of gold precursor solution the well dispersed nanoparticles were formed. The tea polyphenolic flavonoids also play another role in possible capping mechanism of the gold nanoparticles. Overall this whole process was a single step process in a aqueous based medium, without the presence of any harmful chemical or any external surfactant or dispersing agent.

In the following study the same aqueous based tea extract assisted synthesis technique was used to reduce iron salt precursors for the production of iron oxide nanoparticles. In this method the phytochemicals present in tea first does a complex formation with the iron precursor and after reduction of the iron precursor to iron oxide nanoparticles acts as a capping agent for the newly synthesized iron oxide nanoparticles. As the surface of the iron oxide particles are highly reactive especially in aqueous media the encapsulation of the particles by tea functional group helps in stabilization of the particles. Along with the FTIR data and the agglomeration effect observed in microscopic studies we propose that the tea phytochemicals were the main functional groups in reduction and stabilization of iron oxide nanoparticles. The XRD data shows that there are several phases of iron oxide nanoparticles present in the suspension containing $Fe_2O_3$ and $Fe_3O_4$ phases of nanoparticles. The particles have an average dimension between 30-

60 nm and a polydispersed phase. This biogenesis process of iron oxide nanoparticles can be considered cytocompatible as tea is used as a health stimulating beverage in many nations. Thus iron oxide nanoparticles synthesized by this novel route can be used for direct application in biomedical techniques.

| **Characterisation Results** | **Iron Oxide Nanoparticles** | **Gold-Iron oxide Nanoparticles** |
|---|---|---|
| **UV-Vis Spectroscopy** | ~ 300 nm | Red shifts to 560 nm when gold cursor ratio increased |
| **Size** | 30-60 nm | 10-40 nm |
| **Morphology** | Spherical | Spherical |
| **XRD Analysis** | Hexagonal $Fe_2O_3$<br>Rhombohedral $Fe_2O_3$<br>Monoclinic $Fe_2O_3$<br>$Fe_3O_4$ | Cubic gold Nanoparticles<br>$\alpha$-$Fe_2O_3$<br>$\gamma$-$Fe_2O_3$ |
| **Dispersibility** | Highly agglomerated | Slightly agglomerated |

**Table 6.1:** Comparative results of Iron oxide nanoparticles and Gold-Iron oxide composite nanoparticles.

The final study consists of major findings of the work, where the previous two synthesis systems were combined to produce a one-step synthesis technique for fabrication of gold-iron oxide composite nanoparticles. Simultaneous reduction of gold and iron oxide salt precursor by the tea extract at a constant temperature in an aqueous based system produced the Au-$Fe_xO_y$ composite nanoparticles. These particles are reduced, capped and stabilized by the tea phytochemicals. The average size distribution of the composite particles was found to be from 10-40 nm however some particles below 10 nm size distributions were also observed. The Au-$Fe_xO_y$ composite nanoparticles gave an absorption peak which may have red-shifted due to the presence of iron oxide presence as a core material and gold present as a shell material. These two materials may form in the composite structure a non-uniform and incomplete core/shell structure. After heat treatment of the same particles the size of the particles increases to 120-130 nm this might be attributed to the fusing of the iron oxide particles in a ripening process and total encapsulation by the gold nanoparticles as the tea polyphenolic flavonoids acting as the capping and dispersing agents are removed during the heat treatment. The particles also show visible magnetic properties when an external magnetic field is present after heat treatment indicating the conversion of all the $\alpha$-$Fe_2O_3$ phase to $\gamma$-$Fe_2O_3$ or to $Fe_3O_4$ phase, both of which have magnetic properties. The particles with dimensions below 20 nm also indicate presence of particles with super paramagnetic abilities.

It can be concluded that from all the three studies, a green novel route has been developed for synthesizing Au-$Fe_xO_y$ composite nanoparticles, single Au nanoparticles and iron oxide $Fe_xO_y$ nanoparticles. The functional groups present in tea play the major role as reducing agent, capping agent and stabilizing agent. This process can be further optimized to develop a system for one-pot aqueous based synthesis of Au-$Fe_xO_y$ core/shell nanoparticles.

## 6.2 Suggestions for Future Work

The work done here can be further extended and deeply explored. Similar materials can be used for developing other metallic and magnetic nanoparticles by this method. In the future the following works can be done:

1) Similar metallic and magnetic material can be tried with the same plant extract or other plant extract for an aqueous based one-step synthesis procedure and so on.
2) Different cytocompatible solvents or polymers can be used for better dispesibility and stability of the nanoparticles.
3) More detailed studies can be done to explore the new properties of the composite nanoparticles formed.
4) The process can be optimized and the composite nanoparticles can be further studied to explore the possibility of the formation of core/shell nanoparticles using the same one-pot synthesis method.
5) The cytocompatibility of the nanoparticles can be assayed and the structure can be functionalized with other materials as per requirement and application.

# References

Alivisatos A.P. Perspectives on The Physical Chemistry of Semiconductor Nano crystals. J Phys Chem, 1996, 100, 13226–13239.

Alivisatos A.P., Peng X., Wilson T.E., Loweth C.L., Bruchez M.P. Jr., Schultz P.G., Organization of 'nanocrystal molecules' using DNA. Nature. 1996, 382, 609–611.

Alvarez M.M., Khoury J.T., Schaaff T.G., Shafigullin M.N., Vezmar I., Whetten R.L. Optical Absorption Spectra of Nanocrystal Gold Molecules. J Phys Chem B. 1997, 101, 3706-3709.

Amal R., Goon I.Y., Lai L. M H., Lim M., Munroe P., Gooding J.J. Fabrication and Dispersion of Gold-Shell-Protected Magnetite Nanoparticles: Systematic Control Using Polyethyleneimine. Chem. Mater. 2009, 21, 673–681.
Amin, A. and Buratovich, M. The anti-cancer charm of flavonoids: a cup-of-tea will do! Recent Pat. Anti-Cancer Drug Discovery. 2007, 2, 109–117.

Andres R.P., Bielefeld J.D., Henderson J.I., Janes D.B., Kolagunta V.R., Kubiak C.P., Mahoney W.J., Osifchin R.G. Self-assembly of a two-dimensional superlattice of molecularly linked metal clusters. Science. 1996,273,1690-1693.

Ascencio J.A., Raul H.B., Zorrilla C. Production of Iron Oxide Nanoparticles by a Biosynthesis Method: An Environmentally Friendly Route. J. Phys. Chem. C. 2007, 111, 16147-16153.

Bali R., Harris A.T. Biogenic synthesis of Au nanoparticles using vascular plants. Ind Eng Chem Res. 49, 24, 12762–12772.
Bankar A., Joshi B., Ravi K.A., Zinjarde S. Banana peel extract mediated synthesis of gold nanoparticles. Colloids Surf B. 80, 1, 45–50.

Begum, N. A., Mondal, S., Basu, S., Laskar, R., Mandal, D. (2009). Biogenic synthesis of Au and Ag nanoparticles using aqueous solutions of Black Tea leaf extracts. Colloids and surfaces. B, Biointerfaces. 2009, 71, 113–8.

Brust M., Walker M., Bethell D., Schiffrin D.J., Whyman R. Synthesis of thiol-derivatised gold nanoparticles in a two-phase Liquid–Liquid system. J Chem Soc Chem Commun. 1994, 801-802.

Choi S.H., Na H. B., Park Y. I., An K., Kwon S. G., Jang Y., Park M.-H., Moon J., Son J. S., Song I. C., Moon W. K., Hyeon T. Simple and Generalized Synthesis of Oxide−Metal Heterostructured Nanoparticles and their Applications in Multimodal Biomedical Probes. J. Am. Chem. Soc. 2008, 130, 15573–15580.

Chung B.H., Lim Y.T., Cho M.Y., Kim J K., Hwangbo S. Plasmonic Magnetic Nanostructure for Bimodal Imaging and Photonic-Based Therapy of Cancer Cells. Chem. Bio. Chem. 2007, 8, 2204–2209.

Curleya S.A., Cherukuri P., Glazer E.S. Targeted hyperthermia using metal nanoparticles. Adv. Drug Delivery Rev. 2010, 62, 339–345.

Edwards J.K., Solsona B., Landon P., Carley A.F., Herzing A., Watanabe M., Kiely C.J., Hutchings G.J. Direct synthesis of hydrogen peroxide from $H_2$ and $O_2$ using Au–Pd/$Fe_2O_3$ catalysts. J. Mater. Chem. 2005, 15, 4595–4600.

Egorova E.M., Revina A.A. Synthesis of metallic nanoparticles in reverse micelles in the presence of quercetin. Colloids Surf A. 168, 1, 87–96.

Elghanian R., Storhoff J.J., Mucic R.C., Letsinger R.L., Mirkin C.A. Large-scale identification, mapping, and genotyping of single-nucleotide polymorphisms in the human genome. Science. 1998, 280, 1077–1082.

El-Sayed M.A. Some Interesting Properties of Metals Confined in Time and Nanometer Space of Different Shapes. Acc Chem Res. 2001, 34, 257-264.

Feldman M.D., Ma L.L., Tam J.M., Paranjape A.S., Cheruku K.K., Larson T.A., Tam J.O., Ingram D.R., Paramita V., Villard J.W., Jenkins J.T., Wang T., Clarke G.D., Asmis R., Sokolov K., Chandrasekar B., Milner T.E., Johnston K.P. Small Multifunctional Nanoclusters (Nanoroses) for Targeted Cellular Imaging and Therapy. ACS Nano. 2009, 3, 2686–2696.

Feynman R.P. There’s Plenty of Room at the Bottom, Caltech Engineering and Science Magazine. 1959.

Friedman, M., Mol. Overview of antibacterial, antitoxin, antiviral, and antifungal activities of tea flavonoids and teas. Nutr. Food Res. 2007, 51, 116–134.

George C., Dorfs D., Bertoni G., Falqui A., Genovese A., Pellegrino T., Roig A., Quarta A., Comparelli R., Curri M. L., Cingolani R. Manna L. Expanding the Genetic Code of an Animal .J. Am. Chem. Soc. 2011, 133, 2205–2217.

Goesmann H., Feldmann, C. Nanoparticulate Functional Materials. Angew. Chem. Int. Ed. 2010, 49, 1362–1395.

Gupta A.K., Gupta M. Synthesis and surface engineering of iron oxide nanoparticles for biomedical applications. Biomaterials. 2005, 26, 3995-4021.

Hasan T., Rai P., Mallidi S., Zheng X., Rahmanzadeh R., Mir Y., Elrington S., Khurshid A. Development and Applications of Photo-triggered Theranostic Agents. Adv. Drug Delivery Rev. 2010, 62, 1094–1124.

Horisberger M., Rosset J., Colloidal gold, a useful marker for transmission and scanning electron microscopy. J. Histochem. Cytochem. 1977, 25, 295–305.

Huang J, Li Q, Sun D, Lu Y, Su Y, Yang X, Wang H, Wang Y, Shao W, He N, Hong J, Chen C. Biosynthesis of silver and gold nanoparticles by novel sundried *Cinnamomum camphora* leaf. Nanotechnology. 2007a, 18, 104-105.

Huang S.H., Gold nanoparticle-based immunochromatographic test for identification of Staphylococcus aureus from clinical specimens. Clin. Chim. Acta. 2006, 373, 139–143.

Huang W.C., Tsai P.J., Chen Y.C. Multifunctional $Fe_3O_4$@Au Nanoeggs as Photothermal Agents for Selective Killing of Nosocomial and Antibiotic-Resistant Bacteria. Small. 2009, 5, 51–56.

Hung W.H., Aykol M., Valley D., Hou W., Cronin S.B. Plasmon Resonant Enhancement of Carbon Monoxide Catalysis. Nano Lett. 2010, 10, 1314–1318.

Jeong U.Y., Teng X.W., Wang Y., Yang H., Xia Y.N. Superparamagnetic colloids: controlled synthesis and niche applications. Adv.Mater. 2007, 19, 33–60.

Jeong Y.Y., Kim D., Yu M.K., Lee T.S., Park J.J., Jon S. Amphiphilic polymer-coated hybrid nanoparticles as CT/MRI dual contrast agents. Nanotechnology. 2011, 22, 155101.

Jha A.K., Prasad K, Kulkarni A.R. Plant system: nature’s nanofactory. Colloids Surf B. 2009, 73, 219–223.

Joerger R, Klaus T, Granqvist C.G. Biologically produced silver-carbon composite materials for optically functional thin-film coatings. Adv. Mater. 2000, 12, 407-409.

Kataoka K., Kumagai M., T. Sarma K., Cabral H., Kaida S., Sekino M., Herlambang N., Osada K., Kano M. R., Nishiyama N. Enhanced in vivo Magnetic Resonance Imaging of Tumors by PEGylated Iron-Oxide–Gold Core–Shell Nanoparticles with Prolonged Blood Circulation Properties. Macromol.Rapid Commun. 2010, 31, 1521–1528.

Keating C.D., Kovaleski K.M., Natan M.J.J. Protein:Colloid Conjugates for Surface Enhanced Raman Scattering: Stability and Control of Protein Orientation. Phys. Chem. B. 1998, 102, 9404–9413.

Kim D., Park S., Lee J.H., Jeong Y.Y., Jon S. Antibiofouling polymer-coated gold nanoparticles as a contrast agent for in vivo X-ray computed tomography imaging. J. Am. Chem. Soc. 2007, 129, 7661–7665.

Kundu S., Panigrahi S., Praharaj S., Basu S., Ghosh S.K., Pal A., Pal T. Anisotropic growth of gold clusters to gold nano cubes under UV irradiation. Nanotechnology. 18, 7, 075712.

Lee S., Yeo K. M., Shin J. Communication Reductive dissolution of $Fe_3O_4$ facilitated by the Au domain of an $Fe_3O_4$/Au hybrid nanocrystal: formation of a nanorattle structure composed of a hollow porous silica nanoshell and entrapped Au nanocrystal. Chem. Commun. 2010, 46, 64–66.

Lee Y., Garcia M. A., Huls N. A. F., Sun S. Synthetic Tuning of the Catalytic Properties of Au-$Fe_3O_4$ Nanoparticles. Angew. Chem., Int. Ed. 2010, 49, 1271–1274.

Leff D.V., Ohara P.C., Heath J.R., Gelbart W.M. Thermodynamic control of gold nanocrystal size: experiment and theory. J Phys Chem. 99, 18, 7036–7041.

Lengke M., Ravel B., Fleet M.E., Wanger G., Gordon R.A., Southam G. Mechanisms of gold bioaccumulation by filamentous cyanobacteria from gold (III)-chloride complex. Environ Sci Technol. 2006, 40, 6304–6309.

Lengke M., Southam G. Bioaccumulation of gold by sulfate reducing bacteria cultures in the presence of gold (I)-thiosulfate complex. Geochimica et Cosmochimics Acta. 2006, 70, 3646-3661.

Levin C.S., Hofmann C., Ali T.A., Kelly A.T., Morosan E., Nordlander P., Whitmire K.H., Halas N.J. Magnetic plasmonic core/shell nanoparticles. ACS Nano. 2009, 3, 1379–1388.

Liao X., Guo J., Wang X., Miao P., Zhang W., Shi B. One-step seeding growth of controllable Ag@Ni core–shell nanoparticles on skin collagen fiber with introduction of plant tannin and their application in high-performance microwave absorption. J. Mater. Chem. 2012, 22, 11933-11942.

Lin C.A., Yang T.Y., Lee C.H., Huang S.H., Sperling R.A., Zanella M., Li J.K., Shen J.L., Wang H.H., Yeh H.I., Parak W.J., Chang W.H. Synthesis, Characterization, and Bioconjugation of Fluorescent Gold Nanoclusters toward Biological Labeling Applications. ACS Nano. 2009, 3, 395–401.

Lin F.H., Doong R.A. Bifunctional Au−$Fe_3O_4$ Heterostructures for Magnetically Recyclable Catalysis of Nitrophenol Reduction. J. Phys. Chem. C. 2011, 115, 6591–6598.

Lin L, Wang W, Huang J, Li Q, Sun D, Yang X, Wang H, He N, Wang Y. Nature factory of silver nanowires: plant mediated synthesis using broth of Cassia fistula leaf. Chem Eng J. 162, 2, 852–858.

Liu J., Xu R., Kaifer A.E. In Situ Modification of the Surface of Gold Colloidal Particles. Preparation of Cyclodextrin-Based Rotaxanes Supported on Gold Nanospheres. Langmuir. 1998, 14, 7337-7339.

Liu, Q., Liu, H., Yuan, Z., Wei, D., Ye, Y. Evaluation of antioxidant activity of chrysanthemum extracts and tea beverages by gold nanoparticles-based assay. Colloids and surfaces. B, Biointerfaces. 2012, 92, 348–352.

Lukman A.I., Gong B., Marjo C.E., Roessner U., Harris A.T. Facile synthesis, stabilization, and anti-bacterial performance of discrete Ag nanoparticles using Medicago sativa seed exudates. J Colloid Interface Sci. 353, 2, 433–444.

Mafune´ F., Kohno J.Y., Takeda Y., Kondow T. 2002. Full physical preparation of size-selected gold nanoparticles in solution: Laser ablation and laser-induced size control. J Phys Chem B. 106, 31, 7575–7577.

Maier S.A., Kik P.G., Atwater H.A., Meltzer S., Harel E., Koel B.E., Requicha A.A.G. Local detection of electromagnetic energy transport below the diffraction limit in metal nanoparticle plasmon waveguides Nat Mater. 2003, 2, 229-232.

Mandal D., Begum N. A., Mondal S., Basu S., Laskar R. A., Biogenic synthesis of Au and Ag nanoparticles using aqueous solution of black tea leaf extracts. Colloids Surf. B. 2009, 71, 113-118.

Mann S. Biomineralization. Bacteria and Midas touch. Nature. 1992, 357, 358- 360.

Menon D., Narayanan S., Sathy B. N., Mony U., Koyakutty M., Nair S. V. Biocompatible Magnetite/Gold Nanohybrid Contrast Agents via Green Chemistry for MRI and CT Bioimaging. Appl. Mater. Interfac. 2012, 4, 251-260.

Meyre M.E., Tre´guer-Delapierre M., Faure C. Radiation induced synthesis of gold nanoparticles within lamellar phases. Formation of aligned colloidal gold by radiolysis. Langmuir. 24, 9, 4421–4425.

Mukherjee P, Ahmad A, Mandal D, Senapati S, Sainkar SR, Khan MI. Fungus-Mediated Synthesis of Silver Nanoparticles and Their Immobilization in the Mycelial Matrix: A Novel Biological Approach to Nanoparticle Synthesis Nano let. 2001, 1, 515- 519.

Nadagouda M.N., Castle A.B., Murdock R.C., Hussain S.M., Varma R.S. In vitro biocompatibility of nanoscale zerovalent iron particles (NZVI) synthesized using tea polyphenols. Green Chem. 2010, 12, 114-122.

Neel L. "Théorie du traînage magnétique des ferromagnétiques en grains fins avec applications aux terres cuites". Ann. Geophys. 1949, 5, 99.

Niemeyer C.M. Nanoparticles, Proteins, and Nucleic Acids: Biotechnology Meets Materials Science. Angew. Chem. Int. Ed. 2001, 40, 4128–4158.

Niemeyer C.M., Ceyhan B., DNA-Directed Functionalization of Colloidal Gold with Proteins. Angew. Chem. Int. Ed. 2001, 40, 3685–3688.

Njagi E.C., Huang H, Stafford L., Genuino H., Galinido H.M., Collins J.B., Hoag G.E, Suib S.L. Biosynthesis of Iron and Silver Nanoparticles at Room Temperture Using Aqueous Sorghum Bean Extracts. Langmuir. 2011, 27, 264-271.

Nune, S. K., Chanda, N., Shukla, R., Katti, K., Kulkarni, R. R., Thilakavathi, S., Mekapothula, S., et al. Green Nanotechnology from Tea: Phytochemicals in Tea as Building Blocks for Production of Biocompatible Gold Nanoparticles. J. Mat. Chem. 2009, 19, 2912–2920.

Okitsu K., Mizukoshi Y., Yamamoto T.A., Maeda Y., Nagata Y. Sonochemical synthesis of gold nanoparticles on chitosan. Mater Lett. 61, 16, 3429–3431.

Pileni M.P. Nanosized particles made in colloidal assemblies. Langmuir 13, 13, 3266–3276.

R. Bardhan, N. K. Grady, J. Cole, A. Joshi and N. J. Halas, Fluorescence enhancement by Au nanostructures: nanoshells and nanorods. ACS Nano. 2009, 3, 744–752.

Sakthivel N. Narayanan K.B. Green synthesis of biogenic metal nanoparticles by terrestrial and aquatic phototrophic and heterotrophic eukaryotes and biocompatible agents. Adv. Colloid Interfac. 2011, 169, 59-79.

Selvakannan P.R., Mandal S., Phadtare S., Gole A., Pasricha R., Adyanthaya S., Sastry M.J., Water-dispersible tryptophan-protected gold nanoparticles prepared by the spontaneous reduction of aqueous chloroaurate ions by the amino acid J. Colloid Interface Sci. 2004, 269, 97–102.

Selvakannan P.R., Mandal S., Phadtare S., Pasricha R., Sastry M., Capping of gold nanoparticles by the amino acid lysine renders them water-dispersible. Langmuir. 2003, 19, 3545–3549.

Serpell C. J., Cookson J., Ozkaya D., Beer P. D. Core@shell bimetallic nanoparticle synthesis via anion coordination. Nat. Chem. 2011, 3, 478–483.

Shankar S.S., Rai A., Ahmad A., SastryM. Rapid synthesis of Au, Ag, and bimetallic Au core-Ag shell nanoparticles using Neem (Azadirachta indica) leaf broth. J Colloid Interface Sci. 275, 2, 496–502.

Shen Y., Lu W., Xie A., Zhang W. Green synthesis and characterisation of super paramagnetic Fe3O4 nanoparticles. J. Magn. & Magn. Mater. 2010, 322, 1828-1833.

Slot J.W., Geuze H. Sizing of protein A collodial gold probes for immunoelectromicroscopy. J. J Cell Biol. 1981, 90, 533-542.

Song JY, Jang HK, Kim BS. Biological synthesis of gold nanoparticles using *Magnolia kobus* and *Diopyros kaki* leaf extracts. Process Biochem. 2009, 44, 1133–1138.

Sun S., Xu C., Xie J., Ho D., Wang C., Kohler N., Walsh E. G., Morgan J. R., Chin Y. E. Au–Fe3O4 Dumbbell Nanoparticles as Dual-Functional Probes. Angew. Chem., Int. Ed. 2008, 47, 173–176.

Tian Y., Tatsuma T. Mechanisms and Applications of Plasmon-Induced Charge Separation at TiO2 Films Loaded with Gold Nanoparticles. J. Am. Chem. Soc. 2005, 127, 7632–7637.

Tsuji T., Kakita T., Tsuji M. Preparation of nano-size particles of silver with femtosecond laser ablation in water. Appl Surf Sci. 206, 1–4, 314–320.

Vali H, Weiss B, Li YL, Sears SK, Kim SS, Kirschvink JL, Zhang CL. Formation of tabular single-domain magnetite induced by *Geobacter metallireducens* GS-15. Proc Natl Acad Sci U S A. 2004, 16, 16121-16126.

Vilela D., Gonzalez C., Escarpa A. Gold-nanosphere formation using food sample endogenous polyphenols for in-vitro assessment of antioxidant capacity. Anal. Bioanal. Chem. 2012, DOI 10.1007/s00216-012-6084-6.

Wang H., Brandl D. W., Le F., Nordlander P., Halas N. J. Nanorice: a Hybrid Nanostructure. Nano Lett. 2006, 6, 827–832.

Wang L. Y., Bai J. W., Li Y. J., Huang Y., Multifunctional Nanoparticles Displaying Magnetization and Near-IR Absorption. Angew. Chem. Int. Ed. 2008, 47, 2439–2442.

Wang S. R., Zhang J., Liu X. H., Guo X. Z., Wu S. H. A General Approach to Fabricate Diverse Noble-Metal (Au, Pt, Ag, Pt/Au)/$Fe_2O_3$ Hybrid Nanomaterials. Chem.–Eur. J. 2010, 16, 8108–8116.

Wei Y. H., Klajn R., Pinchuk A. O., Grzybowski B. A. Synthesis, Shape Control, and Optical Properties of Hybrid Au/$Fe_3O_4$ “Nanoflowers”. Small, 2008, 4, 1635–1639.

Wisian-Neilson P., García-Alonso F.J. Coordination of Poly(methylphenylphosphazene) and Poly(dimethylphosphazene). Macromolecules. 1993, 26, 7156-7159.

Wisian-Neilson P., Neilson R.H. Poly(dimethylphosphazene) and Poly(methylphenyl-phosphazene. Inorg Synth. 1989, 25, 69-70.

Xia D., Luob X., Ninga Q., Lud Q., Yaod K., Liud Z., J. The detection of HBV DNA with gold nanoparticle gene probes. Nanjing, Med. Univ.2007, 21, 207–212.

Xie J., Zhang F., Aronova M., Zhu L., Lin X., Q. Quan M., Liu G., Zhang G. F., Choi K. Y., Kim K., X. Sun L., Lee S., Sun S. H., Leapman R., Chen X. Y., ACS Nano. 2011, 5, 3043–3051.

Xu C., Wang B., Sun S. Dumbbell-Like Au-$Fe_3O_4$ Nanoparticles for Target-Specific Plating Delivery. J. Am. Chem. Soc. 2009, 131, 4216–4217.

Xuan S. H., Wang F., Y. Wang X. J., Yu J. C., Gong X. L., Leung K. C.-F. Hierarchical core/shell $Fe_3O_4$@$SiO_2$@γ-AlOOH@Au micro/nanoflowers for protein immobilization. Chem. Commun. 2011, 47, 2514–2516.

Xuan S. H., Y. Wang X. J., Yu J. C.,Leung K. C.-F. Preparation, Characterization, and Catalytic Activity of Core/Shell $Fe_3O_4$@Polyaniline@Au Nanocomposites. Langmuir. 2009, 25, 11835–11843.

Yadav V, Sharma N, Prakash R, Raina KK, Bharadwaj LM, Prakash NT. Generation of Selenium containing Nano-structures by soil bacterium, *Pseudomonas aeruginosa*. Biotechnology. 2008, 7, 299- 304.

Yu H., Chen M., Rice P. M., Wang S. X., White R. L., Sun S. H. Dumbbell-like Bifunctional Au−$Fe_3O_4$ Nanoparticles. Nano Lett. 2005, 5, 379–382.

Zeng H., Sun S. H. Syntheses, Properties, and Potential Applications of Multicomponent Magnetic Nanoparticles. Adv. Funct. Mater. 2008, 18, 391–400.

Zhang C, Vali H, Romanek CS, Phelps TJ, Liu SV. Formation of single-domain magnetite by a thermophilic bacterium. Am. Mineral. 1998, 83, 1409–1418.

Zhong C. J., Wang L. Y., Park H. Y., Lim S. I. I., Schadt M. J., Mott D., Luo J., Wang X. Shape memory polymers with built-in threshold temperature sensors. J. Mater. Chem. 2008, 18, 2629–2635.

# Curriculum vitae

**ARITRI GHOSH**

E-mail: aritri.ghosh@gmail.com
Contact: +91-9437842676/ 07381850130
Address: Room no – Flat No-3E, Block-B, 588, Swamiji Sarani, Kolkata-700048, West Bengal

**Objective** To produce quality research work through excellence and team work.

**Profile** A student of Master of Technology (M.Tech by research course) from Department of Chemical Engineering, National Institute of Technology, Rourkela, Odisha from July, 2011. Previously studied Bachelor of Technology in Biotechnology from Haldia Institute of Technology, Haldia, West-Bengal from 2006-2010.

**Education** 07.2011-Present **Master of Technology (M.Tech)**
Chemical Engineering CGPA: 8.23/10 (82.3%) (Up to 4th Semester)
National Institute of Technology, Rourkela, Odisha, India
**Dissertation subject**: Green Route Synthesis of Composite nanoparticles.
Supervisor: Dr. Santanu Paria

06.2006-06.2010 **Bachelor of Technology (B.Tech)** Biotechnology
DGPA: 8.4/10 (80.40%) Haldia Institute of Technology, Haldia, West Bengal, India **Thesis title:** Emergence of an Efficient Probiont.
Supervisor: Dr. Rajarshi Banerjee

04.2003-04.2005 **Higher Secondary (12th Grade Exam)**
Marks Obtained: 735/1000 (73.5%)
West Bengal Council of Higher Secondary Education (WBCHSE)
Sakhawat Memorial Govt. Girls' High School, Kolkata, West-Bengal

04.2001-04.2005 **Secondary (10th Grade Exam)**
Marks Obtained: 699/800 (87.5%)
West Bengal Board of Secondary Education (WBBSE)
Bagbazar Multipurpose Govt. Girls' High School, Kolkata, West-Bengal

## Research Experience

| Institution | Project Title | Field | Duration |
|---|---|---|---|
| National Institute Of Cholera And Enteric Diseases, Kolkata | Porin Induced Expression f Toll-Like Receptor 2 on INT-407 and B-2 Cells | Animal Cell Culture, Molecular Biology, Immunology | 05.2009-07.2009<br>2 Months |
| Ghosh Dastidar Institute Of Infertility And Research, Kolkata | Sperm Preparation Techniques In Human Infertility Research | Assisted Reproductive Technology(ART), Immunology | 05.2008-07.2008<br>2 Months |
| Haldia Institute of Technology, Haldia, West-Bengal | Degree Project: Emergence of An Efficient Probiont | Microbiology, Biochemical Assays, Molecular Biology, Bioinformatics | 07.2009-06.2010<br>1 year |
| National Institute of Technology, Rourkela, Odisha | Degree Project: Green route Synthesis of Composite Nanoparticles | Nanotechnology Synthesis and Characterisation by Spectrometry, Diffraction studies and Scattering studies | 07.2011-Present |

**Research Skills**

**Molecular Biological Technique**: PCR, DNA Isolation from plant and animal tissue, Agarose Gel Electrophoresis, SDS-PAGE

**Biochemical Technique**: Protein Estimation, ELISA

**Microscopy**: Bright-field microscopy, Inverted Light microscopy, Scanning Electron Microscopy, Atomic Force microscopy

**Spectroscopy**: UV-Vis spectroscopy, Fluorescence spectroscopy, FT-IR spectroscopy

**Cell Culture Technique**: Animal cell culture and Microbial Cell Culture

**Analysis Techniques**: Flow cytometric analysis (FACS), Colorimetric analysis, Spectrometric analysis, X-ray Diffraction Techniques, Dynamic Light Scattering Technique

**Nanotechnology techniques**: Synthesis and characterization of nanoparticles by chemical and green routes

**Awards and Achievement**

2011 Qualified Graduate Aptitude Test in Engineering (GATE) with 94.44% (Score 418) in Biotechnology discipline

2010 Academic project of B.Tech (Emergence of an Efficient Probiont) received best project of the batch

2009 Summer Intern Project of B.Tech (Porin Induced Expression of Toll-Like Receptor 2 on INT-407 and B-2 Cells) received best summer project of the batch

2003 National Merit Scholarship (Rank 72) in Secondary Examination of WBBSE

**Extra-Curricular Activities**

1997-2003 School representative in Inter-school and State level quiz competition

An active member of school and college cultural committee

An active member of departmental literary society, both wall magazine and departmental magazine "BIOZONE"

Took Training in Recitation from and participated in different cultural meets organised by Jawaharlal Sishu Bhavan, under Nehru Museum Kolkata.

A bookworm by nature and recyclist craftsman at pleasure.

**Personal Details**

**Date of birth**: 06/08/1987
**Gender**: Female
**Languages known**: English, Bengali, Hindi followed by Spanish
**Nationality**: Indian

**Research Publications**

*To be communicated:*

Aritri Ghosh and Santanu Paria. Biogenesis of composite and core/shell nanoparticles.

Aritri Ghosh and Santanu Paria. Synthesis of gold-iron oxide composite nanoparticles using tea extract.